A Critical Analysis of Electronic Density Functionals for Structural, Energetic, Dynamic, and Magnetic Properties of Hydrogen Fluoride Clusters

CHRISTOPH MAERKER,[1,*] PAUL VON R. SCHLEYER,[1] KLAUS R. LIEDL,[2] T.-K. HA,[3] MARTIN QUACK,[3] MARTIN A. SUHM[3]

[1] *Institut für Organische Chemie der Friedrich–Alexander Universität Erlangen–Nürnberg, Henkestrasse 42, D-91054 Erlangen, Germany*

[2] *Institut für Allgemeine, Anorganische und Theoretische Chemie, Leopold-Franzens-Universität Innsbruck, Innrain 52a, A-6020 Innsbruck, Austria*

[3] *Laboratorium für Physikalische Chemie der ETH Zürich (Zentrum), CH-8092 Zürich, Switzerland*

Received 7 September 1996; accepted 27 February 1997

ABSTRACT: We present extensive computational results on density functional calculations for hydrogen fluoride species $(HF)_n$ (with $1 \leq n \leq 6$) and compare them to results from other approaches and experiments, where available. Among the calculated properties we discuss equilibrium structural parameters, vibrational frequencies, electric dipole moments, IR intensities, dissociation energies, barriers for rearrangement by proton tunneling, NMR chemical shifts and spin couplings for ^{1}H and ^{19}F, and magnetic susceptibilities. It is found that density functional (particularly BLYP) and even more so hybrid approaches (particularly B3LYP) provide useful results. However, we show that due to some characteristic deficiencies, these are in general not competitive with more quantitative results from large basis set MP2 calculations. The calculated magnetic properties do not indicate any ''aromaticity'' connected to a hypothetical electronic ring current. *J Comput Chem* **18**: 1695–1719, 1997

*Present address: Laboratoire de Chimie Biophysique, Institut le Bel, Université Louis Pasteur, 4, rue Blaise Pascal, F-67000 Strasbourg, France

Correspondence to: M. Quack; e-mail: quack@ir.phys.chem.ethz.ch

This article includes Supplementary Material available from the authors upon request or via the Internet at ftp.wiley.com/public/journals/jcc/suppmat/18/1695 or http://journals.wiley.com/jcc/

CCC 0192-8651 / 97 / 141695-25

Introduction

Hydrogen fluoride complexes are an ideal testing ground for studies of hydrogen bonding by spectroscopy and by theory.[1–26] Some interesting current questions concern, in particular, structure, thermodynamics and energetics, rovibrational spectra, tunneling dynamics, kinetics, and magnetic properties of larger clusters $(HF)_n$ (with $n \geq 3$). Here, the application of traditional quantum chemical techniques becomes difficult and one may turn to simplified, approximate theoretical techniques.

Density functional methods for electronic structure calculations[27–29] contain semiempirical elements based on properties of atoms and simple molecules. Prior to routine application in a given field such as hydrogen bonding,[30–32] they have to be checked against experiments and more established quantum chemical approaches for some prototype systems at least.[33] Comparison to experiments, while preferable, is often complicated by the influence of nuclear motion.[34] For hydrogen fluoride clusters, an extensive experimental and theoretical study of nuclear motion effects is available.[1–25] Together with *ab initio* quantum chemistry calculations,[12, 17, 22, 35–45] this has helped to establish firm electronic structure properties for these prototype systems of hydrogen bonding, against which density functional theory (DFT) can be compared.

Hydrogen fluoride clusters $(HF)_n$ cover a wide range of hydrogen bond strengths, increasing by about a factor of 2 from the rather weakly bound dimer $(HF)_2$ ($D_0 = 12.7$ kJ/mol, ref. 13) to the important vapor phase constituents $(HF)_{5,6}$.[16] This is due to cooperative effects,[46–48] which are essentially reducible to three-body interactions,[17] but not merely to classical induction.[47, 49] There is a strong preference for 1-dimensional (1-D) hydrogen bond connectivity, with each HF being engaged simultaneously as donor and acceptor.[23] For clusters beyond the dimer, this leads to symmetric ring structures that are essentially free of strain for more than four monomer units and start to pucker beyond about five monomer units. Among the possible isomerization paths, ring opening, ring branching, hydrogen bond rearrangement, and concerted hydrogen transfer have been discussed in some detail.[7, 16, 17, 23, 40, 45, 50, 51] The latter two processes show important tunneling contributions due to the dominance of hydrogen atom motion. Most of these isomerizations involve relatively high energies, the exceptions being hydrogen bond rearrangement in the dimer through a barrier of ≈ 4 kJ/mol,[52, 53] ring opening in the trimer (≈ 13 kJ/mol, refs. 15, 17), and ring puckering in the larger clusters.[16] Nevertheless, they all occur in HF vapor at thermal equilibrium near room temperature, as evidenced by NMR[54, 55] and IR[9, 56] spectroscopy.

Despite numerous efforts over more than 100 years, the quantitative composition of HF vapor is still under debate, although a unified quantitative picture is emerging at least up to moderate pressures.[23] Depending on pressure and temperature conditions, two or three neighboring cluster sizes in the size range $n = 4$–7 can be found in significant amounts together with the monomer and small amounts of dimer. There is no convincing evidence for an outstanding stability of any of these clusters relative to their direct neighbors except for the reluctance of $(HF)_4$ to lose an HF unit.[23] Early evidence for a dominant role of the hexamer[57] seems to be a consequence of model simplification.[58–60] Nevertheless, in some speculations it has been associated with aromaticity, analogous to the benzene case.[57] We will address the question of aromaticity in HF clusters from an NMR viewpoint.

Electronic density functional approaches appear to be very attractive and promising for the study of hydrogen fluoride vapor for a variety of reasons.

Interaction between HF molecules is less dominated by dispersion forces than between most (if not all) other neutral molecules due to the very large ratio of polarity to polarizability. Given the fundamental deficiencies of current density functionals for dispersion interactions,[61] this is encouraging.

The prohibitive scaling of high level *ab initio* methods with the number of electrons limits their application to smaller HF clusters. Because larger clusters play an essential role in the macroscopic properties of hydrogen fluoride vapor,[9, 23, 60] it would be desirable to have a method at hand that scales more favorably with cluster size.

In larger HF clusters, the strong cyclic hydrogen bond pattern provides a low-energy pathway to hydrogen exchange.[23, 40, 45, 51] This leads to fast scrambling of the hydrogen atoms among the fluorine atoms in the gas phase, even below room temperature despite the very strong H—F chemical bond. Such processes are not captured easily by

traditional intermolecular potential models.[62,63] An ''on the fly'' molecular dynamics treatment in the spirit of the Car–Parrinello method[64,65] could provide an attractive alternative, given a satisfactory density functional approach and a suitable quantization of nuclear motion.[66,67] With this approach, condensed phases of HF, such as the poorly understood liquid[62,68,69] and solid-state phase transitions,[70] can also be addressed.[71]

In combination with high level *ab initio* calculations and experimental data, the semiempirical character of density functional methods might be turned into an advantage. For a specific system such as the HF dimer, available free parameters can be fine-tuned to adjust crucial properties accurately to the experiment without losing global correctness.

In the present article, we investigate to which extent various density functional approaches can meet these expectations by critical comparison to experiment and *ab initio* results. For this purpose, we start with traditional atom centered basis set approaches,[72,73] as implemented in the Gaussian92/94[74,75] and DGauss[76] program packages. Plane wave pseudopotential approaches[77,78] have also been applied.[71,79] A critical issue is the extent to which various gradient correction[80,81] and hybrid[82,83] schemes can overcome the serious deficiencies inherent in the simple local density approximation (LDA).[84,85]

During the course of this work, which has accompanied our experimental investigations,[6,8,9,11,12,14–17,22,26] several density functional studies of hydrogen fluoride dimer[86–91] and related systems,[89,92–98] (mostly water clusters,[77,87,99–108]) have appeared. While we can confirm and extend many conclusions from these investigations, the close connection to experiments and extension to larger cluster sizes in the present work provides a much more critical test of the methodology.

Method

FUNCTIONALS

It is well known that the LDA, which adopts electron correlation and exchange from the free electron gas at the appropriate local density,[27,109–111] severely *over*estimates the binding energy of hydrogen bonded systems.[100] This deficiency of the zeroth order approach can be corrected by more sophisticated functionals involving gradients and higher derivatives of the density, largely based on empirical adjustments to atomic and diatomic systems. Conversely, the Hartree–Fock self-consistent field (SCF) approximation (we avoid the usual acronym HF for obvious reasons) lacks explicit electron correlation and typically *under*estimates the binding energy of hydrogen bonded systems. In $(HF)_2$, complex stabilization through electron correlation is minimal [about 3 times less than for $(H_2O)_2$ with very comparable total binding energy[112]] due in part to the exceptionally small polarizability. Hence, in many aspects, the Hartree–Fock approach provides a better zero-order picture than LDA for hydrogen fluoride clusters. While the next higher level in the traditional quantum chemistry framework (MP2) already performs quite well[53] and a currently powerful approach (CCSD(T)) gives excellent results[43,44,53,113] comparable improvements remain to be demonstrated in the less systematic density functional case.

Dynamical electron correlation is significantly overestimated by LDA. There are several attempts to cure this deficiency, but a simple, yet universal solution cannot be expected.[80] We investigated three of the more popular approaches. A gradient correction suggested by Perdew[80] (P) involves final adjustment to the correlation energy of Ne, which is isoelectronic to HF. The unphysical LDA correlation energy of hydrogen is largely reduced. A more recent correlation correction is due to Lee, Yang, and Parr[114] (LYP). It imposes the proper r_{12} cusp condition[28] and is investigated in detail, because it is quite successful for several classes of substances.[72] Occasionally, it has been advocated for hydrogen bonded systems that the gradient correction for dynamical electron correlation may not be so crucial and can be neglected. Thus, dynamical electron correlation is implemented locally, using either the expressions by Vosko, Wilk, and Nusair[110] (VWN) or Perdew and Zunger[111] (PZ). This approach has been quite successful for some systems.[101]

The effect of the fundamentally nonlocal Pauli principle cannot be accurately described in a local density-framework. Thus, in contrast to the Hartree–Fock approach, the atomic exchange energy is underestimated by about 10%.[115] This is a major reason for the dramatic failure of LDA in HF clusters,[116] where exchange effects also play a central role for cooperativity.[117] A semiempirical gradient correction with one adjustable parameter[115] (B) largely removes this deficiency and ensures the

correct asymptotic behavior for large distances. This proves to be quite useful for hydrogen bonded systems. Alternatively, given that the Hartree–Fock SCF approach provides an excellent zero-order description of exchange, it is natural to incorporate it into DFT despite the associated computational overhead. This is done in hybrid methods, which have been advocated by Becke as a half and half approach[83] (BHH) and as a 3-parameter expression[82] (B3). They turn out to be very successful in reactions that involve hydrogen bonding and hydride transfer,[86,98,118–121] fields in which pure density functional approaches are deficient.[94,118,122–124] We will try to assess whether the older BHH (as advocated in refs. 33, 98, 121, 124, and 125) or the B3 approach is more successful in this respect. Thus, a central goal of the present work is to investigate the relative merits of the existing B, BHH, and B3 exchange corrections in combination with the LYP correlation correction, that is, the BLYP, BHHLYP, and B3LYP methods.

Furthermore, we investigated two variants of the B3LYP functional, in which the mixing ratio between Hartree–Fock and Slater exchange is modified from 0.2:0.8 to 0.25:0.75. In the first variant (B3′LYP), 67% instead of 72% of the Becke exchange gradient correction is added and the LYP contribution is kept at 81%. In the second variant (B3″LYP), 65% instead of 72% of the Becke exchange gradient correction is added while the LYP contribution is reduced from 81 to 75%. Similar modifications have been found to be successful for water.[105] While these modified functionals can give a more balanced description of the HF monomer, the improvements are not necessarily reflected in the dimer properties, as we will see.

BASIS SETS

While development of density functionals is partly based on numerical, basis free methods,[81] application to larger systems usually requires finite basis sets.[126,127] Plane wave basis sets in combination with supersoft pseudopotentials[77] are popular in condensed phase research,[64,65,101] but they can also be applied to finite clusters.[77,128] Our results based on such methods[79] suggest that the choice of appropriate pseudopotentials deserves special care[108] and have motivated us to adopt traditional quantum chemical basis sets and all-electron calculations in the present work.

In quantum chemistry, finite atom-centered basis sets are very successful. Here, basis set superposition error (BSSE[129]) and other effects of basis set incompleteness have to be minimized by choosing sufficiently saturated basis sets. In view of the semiempirical character of density functionals, basis set limits are rarely investigated,[91,130] although this would be desirable for comparison with plane wave methods. Rather, medium and large standard[85] or density functional adapted[116,124] basis sets are used in practice.

Initially we used the DGauss[76,131] program to investigate $(HF)_n$ clusters ($n = 1–6$) at the LDA, BP, and BLYP level. In this program, two sets of basis functions [of double and triple zeta (DZ, TZ) valence quality] adapted to density functional studies are provided in combination with several auxiliary basis sets for the expansion of the electron density. While the minimum geometries resulting from such calculations are reasonable, we observed several limitations. Increasing the basis size from DZ to TZ quality leads to large changes in geometry, frequency, binding energy, and concerted hydrogen exchange barrier for the larger clusters. The binding energy trend is qualitatively as expected from BSSE considerations,[132] but geometry, frequency, and barrier height behave opposite to expectation and experience with other calculations. This leads us to the conclusion that at least the TZ basis set implemented in DGauss in combination with the auxiliary basis set is somewhat unreliable for larger HF clusters, while the DZ basis set (abbreviated D- in the extended tables available in the Supplementary Material) is rather small for quantitative work.

More consistent results are achieved with the density functional module of Gaussian92/94,[74,75,85,133] where we used the BLYP, BHHLYP, and B3LYP functionals together with the standard basis sets D95** and 6-311 + G** as well as 6–311 + + G(3*df*, 3*pd*). The latter basis sets should be large enough to preclude qualitative artifacts, such as those observed in conjunction with 6–31G** density functional calculations on $(HF)_2$,[87] although quantitative deficiencies remain.[86] To approach the basis set limit in a systematic (not necessarily most efficient) way and to avoid limitations in the electrostatic and polarizability description, we also carried out some reference calculations with the aug-cc-pVxZ series of basis sets[43] and a mixed aug-cc-pV(T/Q)Z basis ([8*s*5*p*3*d*2*f*/5*s*3*p*2*d*]), which we used in a systematic HF pair potential scan at the MP2-R12 level.[53] Some of these reference calculations were also extended to MP2 and higher levels and are among the largest calculations carried out for $(HF)_n$ clusters. Geome-

tries were optimized using analytical gradients and frequencies were usually calculated with the fine grid option.

MAGNETIC PROPERTIES

While there are a large number of theoretical studies of the magnetic properties of HF monomer at various levels of sophistication,[134–139] HF clusters have not been investigated previously in this context. B3LYP/6–311 + G** optimized geometries have been used for ^{1}H NMR and ^{19}F NMR chemical shift computations both at the SCF and the DFPT (sum over states, density functional perturbation theory)[140] levels using the IGLO approach.[141,142] The standard IGLO-II and IGLO-III basis sets[142,143] (denoted as BII and BIII, respectively)[142] as implemented both in the IGLO and in the deMon–Kohn–Sham (deMon–KS) programs[144] have been used. The IGLO-DFPT calculations employed the nonlocal Perdew exchange-correlation functional[80,145] and a grid size of high resolution (i.e., option radial = 64). Molar magnetic susceptibilities[146,147] χ_m (in ppm cgs/mol) at the IGLO/BII level and nucleus-independent chemical shifts (NICS; in ppm)[148] at the GIAO-SCF/6–31 + G* level[149] were both computed on the B3LYP/6–311 + G** optimized geometries. NICS values are the negative absolute shielding at a point defined by the mean mass-unweighted Cartesian coordinates of the heavy atoms forming the ring. Indirect $^{1}J_{\mathrm{HF}}$ spin–spin coupling constants, which were computed at the SOS-DFPT-IGLO/BIII level[136] using a modified version of the deMon

TABLE I.
Monomer Equilibrium Distance r_{HF}, Permanent Electric Dipole Moment μ, Harmonic Wave Number ω, and Integrated Molar IR Band Strength S.

Method	Realization	r_{HF} / pm	μ / D	ω / cm^{-1}	S / (km mol^{-1})
DFT	6–311++G**-LDA (ref. 86)	93.0	2.02	4012	140
	6–311 + G**-BLYP	93.3	1.96	3941	106
	aug-cc-pV(T/Q)Z-BLYP	93.4	1.78	3914	91
	6–311 + G**-BHHLYP	90.9	2.00	4291	161
	6–311 + G**-B3LYP	92.2	1.98	4099	130
	6–311++G(3*df*,3*pd*)-B3LYP	92.2	1.83	4093	106
	aug-cc-pVTZ-B3LYP	92.4	1.81	4076	111
	aug-cc-pV(T/Q)Z-B3LYP	92.3	1.81	4070	111
	aug-cc-pVQZ-B3LYP	92.2	1.81	4077	111
	aug-cc-pV(T/Q)Z-B3″LYP	92.0	1.82	4110	116
cqc	6–311++G(3*df*,3*pd*)(SCF)	89.7	1.91	4481	159
	aug-cc-pV5Z(SCF) (ref. 43)	89.7	1.88	4473	
	aug-cc-pV5Z + MP2 (ref. 43)	91.8	1.81	4136	
	aug-cc-pV5Z + CCSD(T) (ref. 43)	91.7	1.80	4142	
	aug-cc-pV5Z + aug(F) + CCSD(T) (ref. 158)	91.8		4143	
	TZ2P(*f*,*d*) + CCSD(T) (ref. 44)	91.8	1.82	4157	102.5
	DZP + MP2 (ref. 17)	91.9	1.99	4221	110
	6–311++G(3*df*,3*pd*) + MP2	91.7	1.82	4173	117
	aug-cc-pVTZ + MP2 (ref. 43)	92.2	1.81	4120[a]	121[a]
	aug-cc-pV(T/Q)Z + MP2	92.0	1.81	4121	119
	aug-cc-pVQZ + MP2 (ref 43)	91.9	1.81	4135[a]	122[a]
	[8*s*6*p*2*d*/6*s*3*p*] + MP2 (ref. 17)	91.8	1.82	4143	120
	[3*s*2*p*1*d*/3*s*1*p*] + ACPF (ref. 40)	91.9		4182	88
	[8*s*6*p*2*d*/4*s*1*p*] + CPF (ref. 37)	91.9	1.77	4135	90
Experiment	Refs. 151, 200, and 201	91.7	1.80	4138	102

S is given within the double-harmonic approximation for convenient comparison to literature data; it can be converted to the more fundamental squared transition dipole moment $\langle \mu_{01} \rangle^2$ and the integrated absorption cross section G via $41.624\ \langle \mu_{01} \rangle^2 / D^2 = G / \mathrm{pm}^2 = 16.6054\ (S / (\mathrm{km\ mol^{-1}})) / (\omega / \mathrm{cm^{-1}})$ (ref. 156). The results are given for different approaches (cqc, conventional quantum chemistry), as discussed in the text. Experimental data are corrected for anharmonic zero-point vibration effects and are therefore directly comparable to the predictions (this is not always the case[202]).

[a] This work.

TABLE II.
Planar $(HF)_2$ Minimum Geometry for Different Approaches.

Potential Surface	r_{HF} / pm	r'_{HF} / pm	R_{FF} / pm	θ / °	θ' / °
6−311++G**-LDA (ref. 86)	94.5	93.6	256	10	73
LDA (ref. 89)	95.3		255	8	
aug-cc-pV(T / Q)Z-B	93.4	93.1	287	6	68
6−31++G**-BLYP (ref. 90)	94.7	94.2	276	8	68
6−311+G**-BLYP	94.0	93.6	278	8	65
aug-cc-pV(T / Q)Z-BLYP	94.2	93.7	275	6	71
6−311+G**-BHHLYP	91.5	91.3	272	8	61
6−31+G**-B3LYP (ref. 87)			273	8	67
6−31++G**-B3LYP (ref. 90)	93.5	93.1	273	8	67
6−311+G**-B3LYP	92.9	92.5	275	8	64
6−311++G(3*df*, 3*pd*)-B3LYP	92.9	92.5	273	5	67
aug-cc-pVTZ-B3LYP	93.2	92.7	273	6	68
aug-cc-pV(T / Q)Z-B3LYP	93.1	92.6	273	6	68
aug-cc-pV(T / Q)Z-B3″LYP	92.8	92.3	272	6	68
6−311++G(3*df*, 3*pd*) + MP2	92.3	92.0	274	5	65
aug-cc-pV(T / Q)Z + MP2	92.6	92.3	275	6	68
aug-cc-pVQZ + MP2 (ref. 43)	92.5	92.2	274	6	68
Best *ab initio*[43, 44, 53]	92.2−92.3	92.0−92.1	273−4	7	68−70
Exp.[1]			272(3)	10(6)	63(6)
Exp.[3]				7(3)	60(2)
Best empirical[12, 53, 160]	92.2−92.3	91.9−92.0	273−4	7−8	65−69

R_{FF} is the distance between the F atoms. Monomer bond lengths are denoted r_{HF}, bond angles of the monomer with the FF axis θ. Primed quantities refer to the nonbonded HF in the dimer.

program, are compared to available experimental data.

Results and Discussion

The information in Tables I–XVI concentrates mostly on experimentally accessible quantities to which comparison is made, wherever possible. This usually involves a reliable treatment of nuclear motion effects, which is contained in the best empirical estimates provided at the bottom of the tables. In some cases (particularly Table XIII), comparison is limited to traditional quantum chemistry results. In both cases approximate error bars are given, where available.

We did not explore the complete 3-D manifold spanned by the various basis sets, functionals, and cluster sizes. For the less promising functionals, only a few small basis sets were tried. However, the similarity of basis set trends across the range of functionals still allows for a qualitative assessment in these cases. For a more complete tabulation of results, we refer to the Supplementary Material that accompanies this article.

HF MONOMER

We start with a brief discussion of monomer properties predicted by various methods, because these already reveal some problems that will show up in large HF clusters. Table I summarizes the density functional results together with a selection of other quantum chemistry predictions and experiments. At the LDA level, the HF bond is too long and too soft (see also Supplementary Material). This deficiency is *not* removed by inclusion of gradient correction (B, BP, BLYP). A similar deficiency is found for OH bonds.[106, 150] As we will see, the underestimated monomer bond strength correlates with underestimated barriers for hydrogen transfer and overestimated frequency shifts in HF aggregates. The opposite is true at the Hartree–Fock level.[41, 45] A mixture of exact Hartree–Fock exchange and semilocal DFT seems to remedy the situation, with BHHLYP clearly overshooting and B3LYP falling slightly short of the desired adjust-

TABLE III.
Electronic (D_e) and Harmonically Corrected (D_0^h) Dimer Dissociation Energies with Respect to Separated Monomers.

Potential Surface	D_e / (kJ mol^{-1})	D_0^h / (kJ mol^{-1})
6−311++G**-LDA (ref. 86)	37.4	
LDA (ref. 89)	38.9	
6−311++G**-B (ref. 86)	14.0	
aug-cc-pV(T/Q)Z-B	11.5	
6−31++G**-BLYP (ref. 90)	20.5 (18.4)	
6−311+G**-BLYP	19.7	12.5
aug-cc-pV(T/Q)Z-BLYP	17.4	10.0
D95**-BHHLYP	27.2	19.1
6−311+G**-BHHLYP	22.7	15.2
6−31+G**-B3LYP (ref. 87)	21.3	
6−31++G**-B3LYP (ref. 90)	21.8 (20.0)	
6−311+G**-B3LYP	21.0	13.7
6−311++G(3*df*,3*pd*)-B3LYP	20.2	12.3
aug-cc-pVDZ-B3LYP	19.3	11.9
aug-cc-pVTZ-B3LYP	18.8	11.4
aug-cc-pV(T/Q)Z-B3LYP	18.8	11.3
aug-cc-pVQZ-B3LYP	18.9	
aug-cc-pV(T/Q)Z-B3″LYP	19.1	11.5
6−311++G(3*df*,3*pd*)+MP2	20.7 (17.0)	12.4
aug-cc-pVDZ+MP2 (ref. 43)	19.6 (16.8)	12.2
aug-cc-pVTZ+MP2 (ref. 43)	19.7 (17.7)	12.1
aug-cc-pV(T/Q)Z+MP2	18.8 (17.8)	11.4
aug-cc-pVQZ+MP2 (ref. 43)	19.4 (18.3)	11.9
Best *ab initio*[43,44]	19.2/19.8	—/12.3
Best empirical[12,53,160]	18.9 (2), 19.1 (2)	12.0 (2), 11.7 (2)
Experimental D_0		12.70(1) (ref. 13)

Energies are compared to MP2 benchmarks and best estimates from *ab initio* theory as well as anharmonic empirically adjusted potential energy surfaces that reproduce the experimental (anharmonic) dissociation energy D_0 of ref. 13. Values in parentheses include BSSE correction.

ment in terms of bond length and curvature. The B3LYP functional contains adjustable parameters that we modified to reproduce the experimental minimum and curvature more closely (B3′LYP and B3″LYP, see Method section). In such a refinement, important electrical properties should also be considered. The B3LYP dipole moment and IR vibrational intensity are strongly basis set dependent. For sufficiently extended basis sets, they come close to experimental values.[151] Similar remarks apply to the polarizability,[86,152–154] where hybrid functionals perform better than pure density functionals.[155] As shown in Table I, the improvement in bond length and harmonic frequency achieved with the B3″LYP functional correlates with a slight deterioration of the electrical properties [electric dipole moment μ and integrated band strength S, related to the more fundamental integrated absorption cross section G via $G/\mathrm{pm}^2 = 16.6054\,(S/(\mathrm{km\ mol}^{-1})/(\omega/\mathrm{cm}^{-1}))$, see ref. 156], so that we had to settle for a compromise adjustment. The flexibility of the B3 approach is obviously not sufficient for an empirical match of the most important minimum properties of a single diatomic species. In comparison, the benchmark aug-cc-pV5Z study[43] and other large basis set results[44,157–159] (see also Table I) impressively show what successive refinement of conventional quantum chemistry approaches can achieve. However, the associated effort is substantial and application to large HF clusters is out of reach for such techniques. This provides us with the main impetus for the present density functional study.

HF DIMER

Having explored the limits of different methods for the HF monomer, the dimer is the next species

TABLE IV.
Predicted Harmonic Wave Numbers ω_i / cm^{-1} and Vibrational Shifts $-\Delta\omega_{1,2}$ Relative to Monomer for $(HF)_2$ Compared to Rounded Best Empirical (Conservatively $\pm$20 cm^{-1}) and *ab initio* Estimates and MP2 Benchmarks.

Potential Surface	ω_1	ω_2	ω_3	ω_5	ω_4	ω_6	$-\Delta\omega_1$	$-\Delta\omega_2$
6−311++G**-LDA (ref. 86)	3947	3718	730	292	203	550	65	294
	(181)	(728)	(178)	(137)	(94)	(292)		
6−311++G**-B (ref. 86)	3959	3879	507	194	120	415	29	109
	(117)	(359)	(222)	(149)	(7)	(248)		
6−311++G**-BP (ref. 86)	3935	3795	602	239	162	471	43	183
	(136)	(486)	(195)	(172)	(14)	(245)		
6−311+G**-BLYP	3903	3790	569	215	155	446	38	151
	(127)	(459)	(209)	(142)	(26)	(241)		
aug-cc-pV(T / Q)Z-BLYP	3872	3735	588	233	165	472	42	179
	(114)	(492)	(134)	(151)	(4)	(154)		
D95**-BHHLYP	4262	4164	622	254	182	479	40	138
	(161)	(492)	(194)	(180)	(34)	(256)		
6−311+G**-BHHLYP	4245	4165	570	220	165	462	46	126
	(166)	(525)	(250)	(132)	(41)	(274)		
6−311+G**-B3LYP	4059	3960	574	217	159	457	41	139
	(148)	(485)	(224)	(142)	(34)	(259)		
6−311++G(3*df*, 3*pd*)-B3LYP	4050	3934	599	236	169	505	43	159
	(127)	(499)	(163)	(146)	(7)	(174)		
aug-cc-pVDZ-B3LYP	4019	3884	593	225	167	482	45	180
	(136)	(511)	(149)	(146)	(12)	(166)		
aug-cc-pVTZ-B3LYP	4032	3907	582	233	164	481	45	170
	(133)	(505)	(152)	(152)	(5)	(169)		
aug-cc-pV(T / Q)Z-B3LYP	4028	3906	587	231	168	480	42	164
	(132)	(511)	(152)	(148)	(9)	(168)		
aug-cc-pV(T / Q)Z-B3″LYP	4064	3945	591	233	170	483	46	165
	(137)	(516)	(155)	(150)	(9)	(171)		
6−311++G(3*df*, 3*pd*) + MP2	4132	4046	609	238	166	547	41	127
	(126)	(476)	(168)	(144)	(3)	(174)		
aug-cc-pVDZ + MP2	4038	3938	577	217	159	473	47	147
	(136)	(466)	(154)	(148)	(12)	(175)		
aug-cc-pVTZ + MP2	4081	3986	580	222	160	477	39	134
	(137)	(475)	(152)	(155)	(6)	(173)		
aug-cc-pV(T / Q)Z + MP2	4079	3989	568	218	159	468	42	131
	(134)	(472)	(156)	(147)	(7)	(170)		
aug-cc-pVQZ + MP2	4094	3997	578	220	163	473	41	138
	(139)	(481)	(153)	(150)	(11)	(173)		
Best *ab initio*[44]	4119	4050	567	210	157	458	38	107
	(119)	(427)	(160)	(141)	(25)	(188)		
Empirical SQSBDE / SNB[12, 160]	4100	4050	—	210	150	410	38	88
With adjustment based on refs. 25 and 162	4090	4030					48	108
New empirical[53]	4100	4030	550	210	155	465	38	108
Anharmonic Fundamental (see refs. 53 and 160)	3931	3868	≈ 480	≈ 160	≈ 125	≈ 420 or 380	31	93

Integrated molar IR band strengths S_i / (km mol^{-1}) are given in the double-harmonic approximation in parentheses. Experimentally, the band strength enhancement of ν_1 (ν_2) over the monomer is approximately 20% (300%).[164] The fundamental ν_6 was observed only in the $K = 0 \rightarrow 1$ and $K = 1 \rightarrow 2$ transitions.[203] From this, two different extrapolations to the rotationless fundamentals were made, depending upon treatment of the Coriolis effects in various potentials (380 and 420 cm^{-1}, refs. 12 and 53), with corresponding differences for ω_6 (410 or 465 cm^{-1}).

TABLE V.
Size Dependence of HF Bond Length r_{HF} in the Minimum Geometry of $(HF)_n$ Clusters.

Potential Surface	$n = 1$	$n = 3$	$n = 4$	$n = 5$	$n = 6$
6−311 + G**-BLYP	93.3	95.4	96.7	97.3	
aug-cc-pV(T / Q)Z-BLYP	93.4			98.3	
6−311 + G**-BHHLYP	90.9	92.4		93.6	
D95*-B3LYP				98.3	
6−311 + G**-B3LYP	92.2	94.0	95.1	95.5	95.7
6−311 + + G(3*df*, 3*pd*)-B3LYP	92.2	94.2	95.7	96.3	
aug-cc-pV(T / Q)Z-B3LYP	92.3			96.4	
6−311 + + G(3*df*, 3*pd*) + MP2 (ref. 45)	91.7	93.3	94.6	95.0	
aug-cc-pVTZ + MP2	92.2			95.7	
Best estimate	91.7	93.3	94.4	94.8	94.9

For $n = 3-5$, the minimum geometry has C_{nh} symmetry; for $n = 6$, a slightly puckered S_6-symmetric minimum is typically found. The limit for an infinite (chain or ring) cluster can be estimated around 95−97 pm (refs. 169 and 170) and in a supersonic jet expansion dominated by pentamers and hexamers, r_{HF} is increased by 3−5 pm (ref. 58) relative to the monomer. The best estimates are mostly derived from *ab initio* calculations[17,40] and shifts relative to the monomer are expected to have an uncertainty of less than 20%.

TABLE VI.
Size Dependence of FF Distance R_{FF} / pm in the Minimum Geometries of $(HF)_n$ Clusters.

Potential Surface	$n = 2$	$n = 3$	$n = 4$	$n = 5$	$n = 6$
6−311 + G**-BLYP	278	263	255	252	
aug-cc-pV(T / Q)Z-BLYP	275			248	
6−311 + G**-BHHLYP	272	261		252	
6−311 + G**-B3LYP	275	262	254	251	250
6−311 + + G(3*df*, 3*pd*)-B3LYP	273	259	250	247	
aug-cc-pV(T / Q)Z-B3LYP	273			247	
6−311 + + G(3*df*, 3*pd*) + MP2 (ref. 45)	274	261	252	248	
aug-cc-pVTZ + MP2	275			248	
Best estimate	273.5(±1.0)	259	251	248	247

For $n = 3-5$, the minimum geometry has C_{nh} symmetry, for $n = 6$, a slightly puckered S_6-symmetric minimum is typically found. Experimental data from pentamer / hexamer supersonic jets (253 pm, ref. 58) and the extended solid (248−251 pm, refs. 169 and 204) have to be corrected for vibrational averaging effects. Best estimates derive from spectroscopic data for $n = 2, 3$ and *ab initio* calculations for the larger clusters.[17,40] Their estimated absolute error is about $\pm(n - 1)$ pm, but the size *trend* is more accurate.

TABLE VII.
Size Dependence of Hydrogen Bond Angle θ_{HFF} / ° in the Minimum Geometries of $(HF)_n$ Clusters.

Potential Surface	$n = 2$	$n = 3$	$n = 4$	$n = 5$	$n = 6$
6−311 + G**-BLYP	8	23	11	5	
6−311 + G**-BHHLYP	8	25		7	
6−311 + G**-B3LYP	8	24	12	6	2
6−311 + + G(3*df*, 3*pd*)-B3LYP	5	21	9	4	
6−311 + + G(3*df*, 3*pd*) + MP2 (ref. 45)	5	22	9	4	
aug-cc-pVTZ + MP2	6			4	
Best estimate	7−8	24	12	6	3

See also Table V. Best estimates derive from *ab initio* calculations.[17,40]

TABLE IX.
Size Dependence of Harmonically Corrected Dissociation Energy of $(HF)_n$ Clusters with Respect to Fragmentation into Separate Monomers D_0^h / (kJ / mol).

Potential Surface	$n = 2$	$n = 3$	$n = 4$	$n = 5$	$n = 6$
6−311 + G**-BLYP	12.5	43.4	89.6	128.5	
		[41]	[84]	[120]	
6−311 + G**-BHHLYP	15.2	48.4		132.9	
		[37]		[102]	
6−311 + G**-B3LYP	13.7	45.6	91.4	130.7	
		[39]	[78]	[112]	
6−311 + + G(3*df*, 3*pd*)-B3LYP	12.3	45.1	93.5	133.0	
		[43]	[89]	[127]	
6−311 + + G(3*df*, 3*pd*) + MP2	12.4	43.7	88.3	125.2	
Best D_0^h estimate	11.7	41	83	116	145
Best D_0 estimate	12.7	43.0	84.5	117	146
aug-cc-pVTZ + MP2 D_e	19.7			165.7	
Best D_e estimate	19.1	63	117	161	199

Values in brackets are obtained by linear scaling to the dimer estimate. Best estimates derived from *ab initio* calculations[17,40] and the experiment,[15,22,171] connected by quantum Monte Carlo calculations.[12,171] The error bars are approximately $\pm n$ kJ / mol for $n > 2$ and ± 0.2 kJ / mol for $n = 2$. For more dimer results, see Table III.

to be addressed. This is mainly motivated by the sizeable experimental and theoretical data basis available for this prototype compound.

HF dimer has a planar equilibrium structure in which one HF molecule forms a nearly linear hydrogen bond to the other, which is bent away from the hydrogen bond axis[1,12] (see Figs. 1, 2). The structural results are summarized in Table II and compared to the best *ab initio*[43,44] and empirical[12,160] estimates, the latter involving an accurate deconvolution of the large amplitude zero-point motion. Basis sets of 6−31G** and inferior quality give qualitatively wrong structures[87,90] even for the best density and hybrid functionals and have not been considered. For the larger basis sets investigated here and in other recent work, agreement for the gradient corrected and hybrid density functionals is generally good to excellent whereas LDA fails completely as discussed before (see also the Supplementary Material). There is one subtle but important exception, namely elongation of the hydrogen bonded HF molecule in the dimer. This elongation is grossly overestimated by most density functionals, with the best one (BLYP) still overshooting by 30−40%, if we take the *ab initio* benchmark results from refs. 43 (0.56 pm) and 44 (0.52 pm) as reference values. The performance of B3LYP is slightly better whereas only the BHHLYP functional, which is otherwise less satisfactory, comes close to the reference value. This observation is in line qualitatively with the monomer properties. A noteworthy result for the B3LYP functional is the rapid convergence of structural properties with basis size in the aug-cc-pVnZ series. Not unexpectedly, the MP2 convergence is somewhat slower.[43]

Dissociation energies at the electronic (D_e) and harmonically zero-point energy corrected level (D_0^h) are shown in Table III. They should only be compared to empirical values for large basis sets, but the sequence B < BP < BLYP < B3LYP < B3″LYP < BHHLYP ≪ LDA is rather persistent for different basis sizes. Large basis set calculations (see Table III) indicate that B3LYP and B3″LYP fall within the experimental window for D_e, while BLYP clearly underestimates and BHHLYP slightly overestimates it. We note that the empirical determination of D_e involves a reliable assessment of zero-point energy contributions to the experimental value[4,13] of $D_0 = 12.70(1)$ kJ/mol.[53,160]

Very recently, the ground state energy difference ΔD_0 between the two isotopomers DFHF and HFDF was determined experimentally.[20,161] While the first determination based on photofragment analysis yields 85 cm^{-1},[20] the more recent spectroscopic analysis[161] favors a value of 74.7(5) cm^{-1}. This quantity is sensitive to the librational degrees of freedom of the hydrogen bond in the HF dimer. Its total anharmonic contribution has been estimated to be relatively small,[12,24] around -5 cm^{-1}

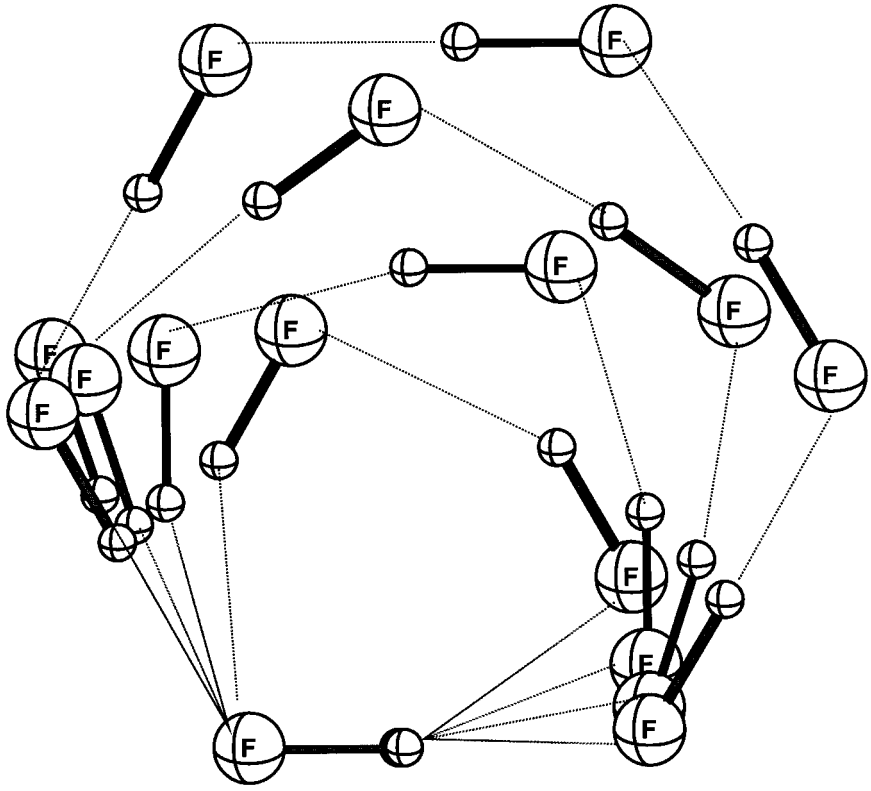

FIGURE 1. Overlaid minimum structures for $(HF)_n$ ($n = 2-6$) at the B3LYP 6−311 + G** level with a common F atom and HF bond vector in the lower left corner.

from the empirically refined SQSBDE potential surface and around -15 cm^{-1} from a new potential surface.[53] While this is certainly the result of a cancellation between different anharmonic effects,[160] it suggests a harmonically determined difference ΔD_0^h of 85(10) cm^{-1} between DFHF and HFDF, due completely to zero-point motion. This may be compared to various theoretical predictions. The SQSBDE prediction of 69 cm^{-1} for ΔD_0^h (ref. 12) (64.16 cm^{-1} for ΔD_0, ref. 24) is somewhat low, presumably due to an underestimation of the in-plane librational frequency for which no experimental results were available. The underlying CPF *ab initio* surface[37] has $\Delta D_0^h = 77.5$ cm^{-1}, in better agreement with the experimental estimate. The MP2 prediction for a saturated basis is estimated to be around 85(5) cm^{-1}, based on 85, 87, 86, and 86 cm^{-1} for the aug-cc-pVxZ basis sets with $x =$ D, T, (T/Q), and Q, respectively. This is in good agreement with the experimentally derived value. Interestingly, the 6−311 + + G($3df, 3pd$) MP2 result of 107 cm^{-1} is clearly too high, suggesting a relatively poor description of hydrogen bond librations in this otherwise quite extended basis set. The B3LYP predictions are less sensitive to the basis set, giving 90 cm^{-1} for the 6−311 + + G($3df, 3pd$) basis, 83 cm^{-1} for the 6−311 + G** basis, and 84 cm^{-1} for the aug-cc-pV(T/Q)Z basis. The B3″LYP result with the aug-cc-pV(T/Q)Z basis is very similar at 85 cm^{-1}. This indicates that the performance of the B3LYP hybrid method is very satisfactory for librations, comparable to that of the MP2 method. The BLYP prediction is $\Delta D_0^h = 78$ cm^{-1} for the aug-cc-pV(T/Q)Z basis, which is also in good agreement with the best experimental estimate within its error bars.

Harmonic frequencies are summarized in Table IV together with IR band strengths in the double harmonic approximation. Here, comparison with the experiments is again complicated by pronounced anharmonic contributions, whose empirical characterization is less complete than for the structural and energetic properties in Tables II and III. The best empirical and *ab initio* estimates for the harmonic properties are given in the table for comparison. Note that for ω_6 and ω_3 the empirical predictions strongly depend on the detailed analysis of a strong Coriolis coupling in various surfaces,[6, 12, 53] but recent combination band spectroscopy[21] supports the higher values that are in

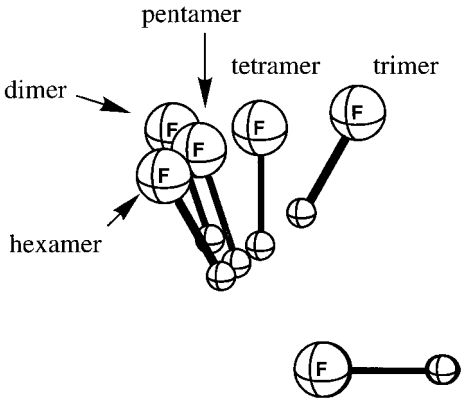

FIGURE 2. Enlarged fragment of Figure 1, illustrating the trend and saturation of the hydrogen bond lengths and angles with cluster size. Notable is the smooth convergence of the cyclic clusters toward a dimerlike, but significantly contracted local hydrogen bond geometry.

good agreement with recent *ab initio* results.[44] The empirical estimates for $\omega_{1,2}$ based on earlier analytical potentials[160] can be adjusted via comparison of 6D- (ref. 25) and (4 + 2)-D (ref. 162) anharmonic calculations with the experiments. This adjustment, which lowers the ω_2 estimate by 20 cm^{-1}, is also given in Table IV. It is supported by results for the most recent analytical potentials,[53] which are also given in the table. From this it is quite clear that the ω_2 frequency is somewhat underestimated at the MP2 level and requires higher levels of electron correlation[44] or empirical adjustment.[53] The experimental results for ω_4 and ω_5 obtained from far IR data[11,12] were recently corroborated by extrapolation from combination band spectroscopy.[163]

Turning now to DFT, Table IV demonstrates a rather satisfactory performance of hybrid functionals as well as of the BLYP density functional for the hydrogen bond vibrational frequencies ω_3–ω_6 within basis set and other limitations discussed above. Given the limitations of the existing empirical data base, it is difficult to discriminate between B, B3, and BHH exchange functionals. In the large basis set limit, all three functionals tend to overestimate the hydrogen bond frequencies somewhat in combination with the LYP gradient correction for correlation. The decreasing overestimation in the sequence BHH > B3 > B should be viewed as an error compensation caused by the decreasing bond strength in the same series (see Table III). It thus seems that the LYP gradient correction intrinsically overestimates the hydrogen bond frequencies to some degree: the hydrogen bond is somewhat too anisotropic. By choosing a medium sized basis set (such as 6–311 + G**), this deficiency becomes less apparent.

In the case of the HF stretching frequencies $\omega_{1,2}$, it is best to focus on shifts $-\Delta\omega_{1,2}$ relative to the monomer, that is, to subtract the monomer deficiencies of various methods. While the smaller ω_1 shift of the acceptor HF is described well by most of the gradient corrected and hybrid functionals, the bonded HF shift $-\Delta\omega_2$ is clearly overestimated by all functionals, even compared to the MP2 level, which by itself overestimates $-\Delta\omega_2$ somewhat. This is in part connected to the overestimate of the HF bond length. Along the sequence BP > BLYP > B3LYP > BHHLYP, the error decreases significantly but it remains notable. The good performance of the B functional (without gradient correction for correlation) is due to error compensation, as evidenced in the preceding tables. HF frequency shifts are of central importance for the identification of larger HF clusters.[16,22,23] An improved density functional would clearly be useful in this context and might be found with a correct description of dispersion forces.[61] Intensity aspects are described satisfactorily by most gradient corrected approaches, given the sparsity of quantitative experimental information[164] and the lack of knowledge about anharmonic contributions.

HF OLIGOMERS

For HF clusters beyond the dimer, density functional approaches become potentially competitive with state of the art *ab initio* approaches due to their much more favorable scaling with system size. Quantitative experimental data to verify this expectation have become available in recent years.[15,16,22,23,165] Rather than discussing the individual cluster sizes one by one, the following tables and Figures 1 and 2 will present size trends.

Qualitative structure predictions are remarkably consistent between different approaches. The cluster size trend is visualized in Figures 1 and 2. One can see that the hydrogen bond geometry of the dimer initially becomes severely distorted with ring formation. With decreasing ring strain, it is more or less recovered, with the notable exception of a significantly shorter hydrogen bond length. For the hexamer minimum structure, DFT supports the presence of slight S_6-symmetric ring puckering previously predicted at the DZP MP2 level[16] (see Fig. 3), although the barrier to pla-

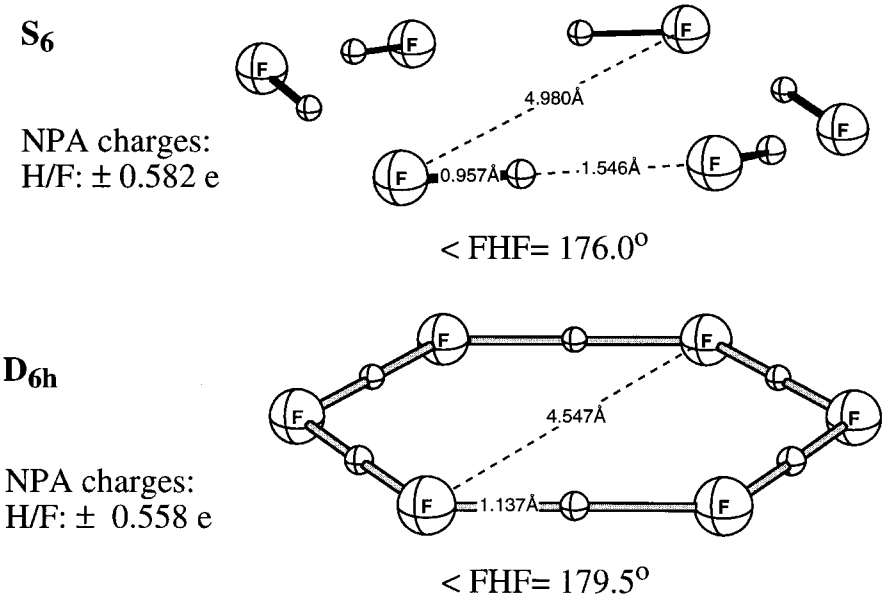

FIGURE 3. Minimum (top, S_6, very close to planar) and concerted exchange saddle (bottom, D_{6h}) structures for $(HF)_6$ at the B3LYP 6−311 + G** level with indication of interatomic distances, angles, and atomic charges (from natural population analysis, NPA; ref. 205).

narity is too small (< 1 kJ/mol) to make safe statements. Single point calculations at higher levels also remain inconclusive. It appears that the potential surface is extremely flat along the puckering coordinates, giving $(HF)_6$ some extra stability at finite temperatures. Experimentally, it will be difficult to distinguish between a quasiplanar and a planar structure.[16] The smaller clusters are clearly planar at equilibrium, but increasingly floppy with respect to the out of plane distortion. For larger clusters, there are several possibilities for isomerism including branched[22, 23, 166, 167] as well as sandwiched, knotted, or folded structures.[23] Because this isomerism is sensitive to much weaker intermolecular interactions than hydrogen bonding (evidenced by the unusually high compressibility of the liquid phase[168]) we defer its investigation via DFT to future progress in the treatment of dispersion forces.

The high (C_{nh}) global minimum symmetry for $(HF)_n$ [n = 3–5(6)] reduces the number of structural parameters to three. Table V shows the HF bond length r_{HF} as a function of cluster size. Its elongation with increasing cluster size is far too large for the LDA approach (≈ 15 pm for the hexamer compared to experimental values of 3–5 pm in the solid[169, 170] and 3–5 pm obtained in a supersonic jet expansion dominated by pentamers and hexamers[58]). Gradient correction and in particular Hartree–Fock admixture reduce this range down to a value that is more consistent with experimental data and *ab initio* results, but still somewhat large except for the BHHLYP functional. Our best estimate for the monomer elongation in the pentamer and hexamer is 3–4 pm. The hydrogen bridged FF distances for gradient and hybrid corrected functionals shown in Table VI are in good agreement with the best estimates from spectroscopy[15] and *ab initio* calculations,[17] provided the basis sets are sufficiently extended. The hydrogen bond angles decrease from 24° in the trimer to 3° in the hexamer by about a factor of 2 for each added monomer unit (see Table VII). This suggests that ring strain is largely released beyond $n = 4$ and that the preferred angle becomes smaller than in the dimer due to cooperative bond strengthening.

Energetic trends can be affected substantially by BSSE, as was demonstrated for the dimer. For *ab initio* treatments, this problem is probably best dealt with by a partitioning of the total interaction energy into one-body, pairwise, and three-body contributions,[171] because the dominant source of BSSE is pair interaction.[17] Therefore, scaling of the *pairwise* part of the dissociation energy to the well-known dimer value[13, 160] has proven quite successful.[17, 23] Studies of BSSE in density functionals are available.[90, 91, 99, 103] They indicate that beyond a certain basis size, the BSSE problem is significantly alleviated whereas it can be large for

small basis sets. In the absence of more detailed knowledge, we scale the total dissociation energy to the experimental dimer value as a first crude guess. Unscaled and scaled results for the electronic binding energy can be found in the Supplementary Material (Table VIII), whereas harmonically zero-point energy adjusted results using an analogous scaling factor are given in Table IX. One can see that scaling removes a large fraction of the enormous discrepancy between different density functional approaches and different basis sets. The good performance of the BLYP approach with the 6−311 + G** basis is partly lost when the basis set is increased to aug-cc-pV(T/Q)Z. Results for the B3LYP functional are also not very uniform across the range of basis sets investigated. In both cases, the dimer binding energy changes significantly while binding in the larger clusters remains largely unaffected. In the complete basis set limit, both BLYP and B3LYP appear to somewhat overestimate binding in the larger clusters, while BLYP at the same time underestimates dimer binding.

It should be emphasized that the best estimates for binding energies given in Tables VIII and IX are the result of a combined spectroscopic, quantum dynamical, and *ab initio* electronic structure calculation effort.[5,12,15,16,22,40,165,171,172] For the dimer, direct combination of spectroscopic dissociation energies D_0^0 (refs. 4, 13, and 20) with anharmonic zero-point corrections is available.[12,53] In other cases one relies on predicted vibrational excitation-fragmentation coincidences, such as in $(DF)_3$ refs. 15, 17 and possibly in $(HF)_4$,[22,23] see also an analogous recent prediction for the water trimer.[173] In larger hydrogen bonded systems with low-lying electronic excitations, one can explore such coincidences quite systematically via pump and dump methods.[174] Presently, the estimated uncertainty in electronic $(HF)_n$ binding energy D_e increases with increasing cluster size, from about 0.2 kJ/mol in the dimer case to about n kJ/mol for larger n-mers. Reference calculations at the MP2 and CCSD(T) levels for nearly complete basis sets such as those carried out for the dimer[43,44] would be highly desirable for the larger clusters.

From the large set of harmonic frequencies, we will only discuss those that are experimentally relevant, either through IR activity or because of their role in concerted hydrogen exchange. Table X summarizes the IR active (degenerate) and totally symmetric HF stretching wave number shifts. The former play a central role in the cluster size identification in static cell[9,23,56] and supersonic jet measurements.[16,22,165,171,172] The opposing role of anharmonicity and zero-point motional weakening on these shifts has been discussed in detail.[22,53] It remains unclear whether locally harmonic predictions should under- or overestimate the observed shifts. For large clusters, anharmonicity is likely to dominate, leading to a slight underestimation of $-\Delta\nu$ by $-\Delta\omega$.[22] For small clusters, the opposite situation is predicted.[53] In any case, a rather close similarity between the two due to compensation of the above-mentioned nonlocal effects is expected.[16,22] This is reflected in the MP2 results at the DZP level, although a substantial amount of basis set incompleteness remains at this level. We should note that the experimental frequency shifts are still under debate,[22,165] but the set favored by us (see Table X) is on the large side. The shifts predicted by DFT are even larger, in line with the observations for the dimer. Based on these results, the BLYP functional will only have a limited predictive power for mid-IR spectroscopy, although it

TABLE X.
Harmonic IR-Active / Totally Symmetric HF Stretching Wave Number Shift $-\Delta\omega$ / cm^{-1} as Function of Cluster Size.

Potential Surface	$n = 3$	$n = 4$	$n = 5$	$n = 6$	$n = 7$
6−311 + G**-BLYP	346 / 472	602 / 812	736 / 961		
6−311 + G**-BHHLYP	250 / 342		553 / 710		
6−311 + G**-B3LYP	297 / 406	529 / 710	660 / 854		
6−311 + + G(3*df*, 3*pd*)-B3LYP	344 / 475	660 / 896	816 / 1068		
DZP + MP2 (ref. 17)	247 / 359	472 / 659	599 / 796	660 (474) / 834	695 / 843
6−311 + + G(3*df*, 3*pd*) + MP2	280 / 396	554 / 755	686 / 895		
Anh. experiment	249 / —	516 / —	661 / —	716 / —	746 / —

For the $(HF)_6$ S_6 structure, the puckering-induced weak IR satellite band is given in parentheses.

may be rendered useful through scaling. Hybrid functionals perform better. This is particularly true for BHHLYP, whereas B3LYP also overestimates the shifts.

The second frequency shift shown in Table X refers to the lowest, totally symmetric HF stretching mode, which is Raman active. No experimental data are available for this vibration, although they could shed much light into the remaining open questions on HF vapor. If one is willing to accept the MP2 results as a reference, then the conclusions for the IR-active stretch are transferable to the totally symmetric mode, because the shift ratio remains similar throughout the investigated levels of theory.

Turning to hydrogen bond vibrations, the situation seems to be more favorable for DFT, perhaps partly because experimental information on harmonic frequencies remains rather uncertain and indirect. Table XI summarizes the IR-active in- and out of plane libration fundamentals, which are in satisfactory agreement with experimental and *ab initio* estimates for gradient corrected and hybrid functionals. The same applies to the FF stretching modes given in Table XII, of which one is IR active[23] and the other one has been assigned in combination with the HF stretching fundamental.[22,23]

The good performance of gradient corrected density and hybrid functional approaches close to the hydrogen bond minimum (except for HF stretch related issues) does not guarantee a reliable performance in other more elevated regions of the potential energy surfaces.[98,105] One obvious and very important region that has been investigated in some detail is the transition state for concerted hydrogen transfer[40,45,50,175] in cyclic HF clusters. The only experimental estimate for the corresponding barrier comes from NMR spectroscopy,[54,55] where the ^{19}F and ^{1}H doublets are found to coalesce even in dilute cold vapor due to the rapid exchange of hydrogen between the fluorine atoms

TABLE XI.
Harmonic IR-Active In-Plane / Out of Plane HF Libration Wave Numbers ω_{lib} / cm^{-1} as Function of Cluster Size.

Potential Surface	$n = 3$	$n = 4$	$n = 5$	$n = 6$
6−311 + G**-BLYP	619 / 714	866 / 787	950 / 775	
6−311 + G**-BHHLYP	558 / 699		893 / 772	
6−311 + G**-B3LYP	589 / 707	841 / 787	934 / 780	
6−311 + + G(3*df*, 3*pd*)-B3LYP	633 / 733	942 / 855	1040 / 865	
6−311 + + G(3*df*, 3*pd*) + MP2	581 / 719	903 / 859	1007 / 873	
Best harmonic	600 / 700	850 / 800	950 / 800	700−1000
Anh. experiment, $n = 5-6$			≈ 600−900 [23]	

For the nonplanar $(HF)_6$ S_6 structure, the range of IR-active librations is given.

TABLE XII.
Harmonic IR-Active / Totally Symmetric FF Stretching Wave Number ω_{FF} / cm^{-1} as Function of Cluster Size *n*.

Potential Surface	$n = 3$	$n = 4$	$n = 5$	$n = 6$
6−311 + G**-BLYP	200 / 220	277 / 209	272 / 179	
6−311 + G**-BHHLYP	195 / 229		256 / 181	
6−311 + G**-B3LYP	198 / 223	271 / 210	267 / 180	
6−311 + + G(3*df*, 3*pd*)-B3LYP	205 / 228	299 / 224	300 / 197	
6−311 + + G(3*df*, 3*pd*) + MP2 (ref. 45)	190 / 215	278 / 210	279 / 186	
Best harmonic	200 / 220	280 / 210	270 / 190	250 / 175
Anh. experiment, $n = 4 \rightarrow 6$			≈ 260 → 230 [23] / ≈ 185 → 150 [22]	

For the $(HF)_6$ S_6 structure, only the dominant component is given. Anharmonic experimental values for $n = 4 \rightarrow 6$ are approximate and below the best harmonic estimate, which is derived from *ab initio* and analytical potential energy surfaces.[17]

and among the clusters. The lower limit for the rate constant has been converted to a barrier height of less than 48 kJ/mol under very simplifying assumptions,[55] neglecting in particular differences in the partition function of activated complex and ground state cluster. Based on the dominance of pentamers and hexamers and corresponding *ab initio* information, we can tighten this upper barrier limit to < 39 kJ/mol, neglecting anharmonic and tunneling contributions. It should be emphasized that steps other than the concerted exchange, such as cluster formation and dissociation, may become rate limiting in diluted vapor. In any case, an experimental lower bound for the barrier is not available, but the absence of any indication for tunneling splittings in the IR spectra seems to exclude extremely low barriers. Rough estimates of the ground state tunneling splitting based on 2-D coupled HF/FF stretch motion in *ab initio* potentials indicate tunneling splittings below 0.01 cm^{-1} in the vibrational ground state, with strong promotion through FF stretch excitation, as discussed qualitatively in ref. 45. In such a situation, density functionals are both potentially useful and difficult to judge. Table XIII summarizes our exploratory approach to this question at the MP2 as well as at various density and hybrid functional levels, together with available high level benchmark calculations. Hartree–Fock results will not be discussed, because they overestimate the barrier substantially[35,41,45] (see, however, ref. 176).

The D_{nh} saddle point structures are predicted very uniformly across the variety of methods and there is little doubt about the reliability of these results. Figure 3 illustrates the $(HF)_6$ case, where slight puckering may further lower the energy by a small amount. The general trends with cluster size have been discussed elsewhere[40,45] and can be summarized as an increasingly linear and relaxed F-H-F arrangement. However, the bandwidth of energetic predictions is enormous. Apart from a general trend toward smaller barriers up to about $(HF)_5$ (refs. 16, 175), despite the increasing number of hydrogens that have to be moved, there is little convergence between different approaches, coupled with a strong basis set dependence. For comparison with the experiment, it is most sensible to look at zero-point energy corrected barriers in the spirit of transition state theory or 1-D reaction coordinate tunneling models. This means that the difference in (here only harmonic) zero-point energy of the transition state (with contributions from all modes except for the reaction coordinate) and the ground state (for all modes) is added to the electronic barrier. Due to the strong harmonic curvature of the reaction coordinate, this can give rise to apparently negative barriers in cases where the electronic energy barrier is small (see the LDA results in the Supplementary Material). Such a result will in part be an artifact of the harmonic approximation, but it can be taken as strong evidence for a vibrational ground state with effectively delocalized protons in the hydrogen bonds.

For comparable basis sets, the sequence of barrier heights appears to be approximately BHHLYP > QCISD(T) ≈ CCSD(T) > MP2 > B3″LYP > B3LYP > BLYP > BP > LDA, where the experimental constraints are only able to exclude LDA, BP, BLYP, and BHHLYP with reasonable probability. Considering the underestimated HF frequency and overestimated HF elongation at the B3LYP level, which tend to lead to an underestimated barrier for exchange, one is tempted to also exclude B3LYP from the range of experimentally consistent predictions. The adjusted B3′LYP (see Supplementary Material) and B3″LYP functionals have somewhat higher barriers, consistent with this correlation between monomer softness and barrier height. Barrier calculations near the basis set limit at MP2 and higher *ab initio* levels remain to be performed before a reliable prediction can be made. The results in the tables show clearly that for barrier heights, the 6−311 + G** basis is still quite far from the basis set limit. Nevertheless, the single-point calculations carried out with this basis set at QCISD(T) (see Supplementary Material) and CCSD(T) level give an indication of the importance of higher order correlation contributions (see also the caption to Table XIII). One should not dismiss the possibility that concerted *n*-proton transfer barriers depend on higher than triple excitation contributions. The best theoretical estimates quoted in Table XIII should be taken as rough guesses only, as far as energetics is concerned. It is interesting to note that beyond $(HF)_3$, the concerted exchange barrier falls well below the threshold for complete dissociation into monomers and becomes competitive with the lowest available dissociation thresholds. In this sense, $(HF)_n$ clusters with $n > 3$ may be regarded as new molecules, even with several isomers, rather than merely as weakly bound HF aggregates. As the excitation energy per monomer required for concerted hydrogen transfer in cyclic HF clusters approaches a positive low limiting value, the excitation energy per cluster must go through a minimum. This minimum is reached near or at the pentamer[16] (see Table XIII), thus adding to the importance of this aggregate

TABLE XIII.
Structure and Energetics of Concerted Hydrogen Exchange Transition State in Cyclic Planar HF Clusters.

Potential Surface	n	r_{HF} / pm	R_{FF} / pm	∠FHF / °	E_B^e	E_B^h	ω_i'
DZP + MP2 (ref. 17)	2	117.9	206	121	174.6	164.3	2306
6−311++G(3*df*,3*pd*) + MP2 (ref. 45)		118.2	206	122	167.4	158.6	2262
[8*s*6*p*2*d* / 6*s*3*p*] + MP2					174	164	
ACPF (ref. 40)		117.8	205	121	185		
QCISD(T) / / MP2 (ref. 51)					186.4	176.3	
6−311 + G**-BHHLYP		117.4	204	121	200.5	188.1	2468
6−311 + G**-B3LYP		119.3	207	120	172.2	160.7	2241
6−311++G(3*df*,3*pd*)-B3LYP		119.1	207	121	157.8	148.4	2203
Best theoretical estimate		118	206	122	170	160	
DZP + MP2 (ref. 17)	3	114.9	223	152	87.7	75.0	1773
6−311++G(3*df*,3*pd*) + MP2 (ref. 45)		115.1	224	154	78.4	66.8	1733
CCSD(T) (ref. 50)					75	61	
ACPF (ref. 40)		114.7	223	153	86.6		
QCISD(T) / / MP2 (ref. 51)					95.4	84.2	
6−311 + G**-BHHLYP		114.4	222	152	104.8	90.9	1917
6−311 + G**-B3LYP		116.1	225	152	81.1	68.5	1705
MP2 / / 6−311 + G**-B3LYP					95.6		
CCSD(T) / / 6−311 + G**-B3LYP					102.0		
6−311++G(3*df*,3*pd*)-B3LYP		116.1	226	153	69.6	57.2	1653
Best theoretical estimate		115	224	153	80	65	
DZP + MP2 (ref. 17)	4	113.6	226	166	61.1	42.5	1526
6−311++G(3*df*,3*pd*) + MP2 (ref. 45)		113.8	226	168	53.3	33.9	1498
ACPF (ref. 40)		113.5	225	167	61.9		
6−311 + G**-B3LYP		114.7	228	167	54.9	36.5	1454
MP2 / / 6−311 + G**-B3LYP					69.3		
CCSD(T) / / 6−311 + G**-B3LYP					75.8		
6−311++G(3*df*,3*pd*)-B3LYP		114.7	228	168	43.6	25.0	1403
Best theoretical estimate		113.5	226	167	55	35	
DZP + MP2 (ref. 17)	5	113.0	226	174	58.1	34.7	1436
6−311++G(3*df*,3*pd*) + MP2 (ref. 45)		113.2	226	177	52.6	27.1	1431
aug-cc-pVTZ + MP2		113.5	227	177	45.7		
6−311 + G**-BLYP		115.5	231	175	40.0	17.9	
aug-cc-pV(T / Q)Z-BLYP		115.8	232	177	30.6		
6−311 + G**-BHHLYP		112.5	225	174	74.9	48.0	1583
6−311 + G**-B3LYP		114.0	228	175	51.6	27.6	1368
6−311++G(3*df*,3*pd*)-B3LYP		114.1	228	176	40.8	17.0	1318
aug-cc-pV(T / Q)Z-B3LYP		114.3	228	176	41.3		
aug-cc-pV(T / Q)Z-B3″LYP		113.9	228	176	44.0		
Best theoretical estimate		113	226	175	50	25	
DZP + MP2 (ref. 17)	6	112.7	225	179	65.5	37.0	1431
ACPF (ref. 40)		112.7	225	179	69.5		
6−311 + G**-B3LYP		113.7	227	179	57.1		
Best theoretical estimate		112.5	225	179	60	30	

Dimer to hexamer, for the hexamer, the planar structure often corresponds to a fourth-order saddle, which is very close to the puckered first-order saddle, however. Electronic (E_B^e) and harmonically corrected (E_B^h) threshold energies are given in kJ / mol. The imaginary wave number along the reaction coordinate $\omega_i' = \omega_i / \mathrm{cm}^{-1}$ is a measure of the reaction profile curvature. Single point calculations at a higher level with the same basis set (where given) are indicated by //. Best energy estimates remain quite uncertain [±(5−10) kJ / mol] in the absence of experimental constraints and large basis set MP2, QCISD(T), and CCSD(T) reference calculations. A very recent explicitly correlated coupled cluster study suggests that E_B^e may be closer to the upper limits estimated here (ref. 206).

size for HF vapor.[23] Obviously, further experimental information on concerted exchange, which seems to fall between the time scales easily accessible to NMR and IR spectroscopy, would be highly desirable. In this context, a poorly understood IR absorption near 1240 cm^{-1} (ref. 23) may be of interest.[177]

MAGNETIC PROPERTIES

Chemical Shifts

In their historical article dealing with the effects of association of hydrides on chemical shifts, Schneider et al. concluded that ''The proton signals measured in the liquid state near the melting point, which correspond to maximum association, show large shifts to lower magnetic field relative to the corresponding gas signals.''[178] The estimated ^1H NMR gas to liquid shift of hydrogen fluoride was 6.65 ppm after diamagnetic bulk susceptibility (1.05 ppm) and other corrections were applied.[178] The ^1H NMR chemical shift differences between monomeric HF in the vapor and liquid HF reported by two groups, 4.35 ppm (ref. 55) and 5.72 ppm (ref. 54), are not in good agreement. The ^1H NMR chemical shift of hexameric HF in the vapor was reported to be 1.20 ppm (ref. 55) downfield from liquid HF (all data including a bulk susceptibility correction of 0.85 ppm). Hence, the relative ^1H chemical shift of the HF hexamer should be 5.6–6.9 ppm downfield from the monomer in the gas phase, although there is additional uncertainty in the gas phase model employed in ref. 55. Computed ^1H NMR chemical shielding constants at IGLO/BII and at IGLO-DFPT/BIII (Table XIV) agree, although the calculated chemical shift differences between monomer and hexamer (S_6) [7.9 ppm (IGLO/BII) and 8.2 ppm (IGLO-DFPT/BIII)] are outside the experimental range.[54, 55, 178]

Similarly, the reported upfield ^{19}F NMR shifts of monomeric HF in the gas phase range from 14.0 to 20.5 ppm (refs. 54, 55) versus liquid HF (both values corrected by 0.85 ppm for the bulk diamagnetic susceptibility). In contrast, the ^{19}F NMR chemical shift of hexameric HF in the vapor is $\approx$ 2.45 (ref. 55) downfield from liquid HF (same bulk susceptibility correction applied). Correlated IGLO-DFPT/BIII computations give a theoretical chemical shift difference of 29.3 ppm between the monomer and the S_6 symmetric hexamer, compared with the 16.5–23 ppm experimental range. Although the IGLO-DFPT/BIII level overestimates the deshielding effect, it is superior to SCF levels.[179] The use of other exchange-correlation functionals like that of Perdew and Wang (PW91)[180] gave similar results as the Perdew E_{XC} functional (Table XIV). Vibrationally averaged chemical shift calculations remain to be done for these prototype hydrogen transfer systems and could give rise to interesting isotope effects.[181] Recent GIAO-CCSD and GIAO-CCSD(T) calculations by Gauss and Stanton on the HF monomer, employing rather large $pz3d2f/pz3p$ basis sets,[138] are in quantitative agreement with the experimentally derived equilibrium shieldings σ_e of 29.2 ppm for ^1H NMR and 419.7 ppm for ^{19}F NMR (Table XIV).[182]

Are $(HF)_n$ Species Cyclically Delocalized?

The ''aromaticity'' of the symmetrical D_{6h} (H_6) transition state for the exchange of three H_2 molecules has been assessed recently by applying energetic and magnetic criteria. The ''energy of concert'' is quite large, 37.2 kcal/mol versus $2H_2 + 2H$.[183] The magnetic susceptibility enhancement Λ (−9.4) of H_6 (D_{6h}) (ref. 183) is comparable to the corresponding benzene value of −13.4 (all data at IGLO/BII and in ppm cgs/mol, for unit conversion see caption to Table XV).[184] The computed molar magnetic susceptibility anisotropy $\Delta\chi_{\text{anis}}$ of H_6 (D_{6h}) (−21.7) is only one-third of that for benzene (−62.9),[184] but it is quite negative compared with $\Delta\chi_{\text{anis}}$ of H_2 (−0.3 ppm cgs/mol).[183] Although other H_n rings with $4m + 2$ σ-electrons were also indicated to be aromatic, based on the same criteria, these species are highly artificial species with more than one imaginary frequency.[183] In this context we were interested in whether the HF oligomers and their transition states would show evidence for any cyclic delocalization. Specifically $(HF)_3$ has six bonding electrons in the ring plane as well as six π electrons. Do the $(HF)_4$ and $(HF)_6$ rings with $4m$ electrons show the opposite behavior?

In fact, no alternation with ring size and no clear-cut evidence for cyclic delocalization was found in any of the $(HF)_n$ rings or their transition states (Table XV). The absolute χ_m values for monomeric HF, computed either at IGLO/BII, local DFT,[135] SCF, or MP2 levels[185] of theory for an isolated molecule, are in good mutual agreement but slightly exceed the liquid phase experimental value of −8.6 ppm cgs/mol.[186] The susceptibility

TABLE XIV.
Computed ^{19}F and ^{1}H NMR Isotropic Equilibrium Shielding Constants σ_e (ppm).

Compound		σ ^{19}F	σ ^{1}H	σ ^{19}F	σ ^{1}H
$(HF)_1$ (exp)	$C_{\infty v}$			419.7 ± 0.3[a]	29.2 ± 0.5[a]
		IGLO / BII		IGLO-DFPT / BIII	
HF	$C_{\infty v}$	386.6 (0.0)	28.0 (0.0)	405.5 (0.0)	29.7 (0.0)
				408.0[b]	29.2[b]
				418.1[c]	29.1[c]
				418.6[d]	29.2[d]
$(HF)_2$	C_s, H_b	397.8 (−11.1)	25.7 (2.3)	406.1 (−0.6)	27.2 (2.5)
	C_s	388.5 (−1.8)	26.7 (1.3)	395.4 (10.1)	28.3 (1.3)
	C_{2h}	388.5 (−1.9)	17.0 (1.0)	392.4 (13.1)	28.6 (1.1)
	D_{2h}	268.2 (118.5)	11.1 (16.9)	248.2 (157.4)	14.2 (15.4)
$(HF)_3$	C_{3h}	387.6 (−1.0)	24.1 (4.0)	377.7 (27.9)	25.2 (4.5)
	D_{3h}	346.3 (40.4)	11.2 (16.8)	316.4 (89.2)	13.6 (16.1)
$(HF)_4$	C_{4h}	387.9 (−1.3)	21.6 (6.4)	374.0 (31.6)	22.8 (6.9)
	D_{4h}	354.4 (32.3)	10.8 (17.2)	324.3 (81.3)	13.2 (16.5)
$(HF)_5$	C_{5h}	389.0 (−2.3)	20.5 (7.5)	374.4 (31.2)	21.8 (7.9)
	D_{5h}	359.8 (26.9)	10.6 (17.4)	331.0 (74.6)	13.1 (16.6)
$(HF)_6$	S_6	390.0 (−3.4)	20.1 (7.9)	376.2 (29.3)	21.5 (8.2)
	C_{6h}	390.2 (−3.6)	20.1 (7.9)	376.4 (29.1)	21.5 (8.2)
	D_{6h}	362.7 (23.9)	10.6 (17.5)	335.8 (69.8)	13.1 (16.6)

[a] Reference 182.
[b] Employing the Perdew–Wang exchange-correlation functional (PW91).
[c] GIAO-CCSD values from ref. 138.
[d] GIAO-CCSD(T) values from ref. 138.
All IGLO-DFPT / BIII calculations employed the Perdew exchange-correlation functional, if not noted otherwise. Relative chemical shifts (ppm) of the HF oligomers with respect to monomeric HF given in parentheses.

exaltation Λ of the HF oligomers, taken relative to the susceptibility χ_m of the same number of monomeric HF, is quite small even for the D_{3h} $(HF)_3$ transition state. Thus, there is no diamagnetic susceptibility exaltation. Furthermore, the molar magnetic susceptibility anisotropies $\Delta\chi_{\text{anis}}$ are very small and also point to the absence of diatropic ring currents.

We further applied the newly developed NICS probe,[148] which has been shown to correlate well with several other aromaticity criteria.[148] The NICS value for the D_{nh} symmetric HF oligomers (n = 3–6) show (Table XVI), with the exception of the trimer, only very little change with respect to the corresponding C_{nh} symmetric ground states. Because NICS decreases with increasing ring size, the larger values for the trimer may be due to the proximity of the σ bonds rather than ring current effects. In contrast, H_6 (D_{6h}) and benzene have NICS values of −24.2 (ref. 187) and −9.7 ppm,[183] respectively. We relate the absence of ring current effects in HF oligomers to the highly ionic bonding in the rings; for example, note the large atomic charges (ca. $\pm 0.58e$), even in the cyclic ground states (Fig. 3).

In summary, these magnetic criteria suggest that the cyclic HF oligomers [$(HF)_n$, n = 3–6] do not exhibit delocalization either in their C_{nh} symmetric ground states or in their D_{nh} symmetric transition structures for concerted proton exchange. Possible magnetic susceptibility contributions from hydrogen (proton) motion (e.g., in a circular tunneling process) are not taken into account in the calculations, but might be of some general interest.

$^{1}J_{HF}$ Indirect Spin–Spin Coupling Constants

The computed $^{1}J_{HF}$ in HF monomer, 380 Hz (at SOS-DFPT-IGLO/BIII//B3LYP/6–311 + G**, using the Perdew E_{XC} functional),[188] varies nonmonotonically in the oligomers (to 395 Hz in the S_6 hexamer), with a minimum $^{1}J_{HF}$ of 373 Hz in the C_{3h} symmetric trimer. The measured $^{1}J_{HF}$ in gaseous HF, 529 ± 23 Hz,[189] is much greater. Malkin et al. attributed the discrepancy for monomeric HF to underestimation of the Fermi-

TABLE XV.
Analysis of IGLO / BII / / B3LYP / 6 – 311 + G Computed Molar Magnetic Susceptibilities χ_m of $(HF)_n$ Clusters (n = 1 – 6).**

Species		χ_{11}	χ_{22}	χ_{33}	$\Delta\chi_{anis}$[a]	χ_{dia}	χ_{para}	χ_{nl}	χ_m	Λ[b]
HF	$C_{\infty v}$	−10.58	−10.58	−10.21	0.37	−8.39	−1.75	−0.32	−10.46	0.00
					0.61[c]				−11.22[c]	
					0.52[d]				−10.91[d]	
					0.52[e]				−10.40[e]	
					0.54[f]				−10.78[f]	
									Liquid −8.6[g]	
$(HF)_2$	C_s	−20.81	−20.76	−21.11	−0.33	−16.85	−3.48	−0.57	−20.90	0.02
	C_{2h}	−20.59	−20.99	−21.05	−0.26	−16.87	−3.56	−0.55	−20.88	0.04
	D_{2h}	−21.07	−20.01	−17.61	2.93	−17.86	−2.18	0.48	−19.56	1.36
	$C_{\infty v}$	−21.18	−21.18	−20.44	0.74	−16.85	−3.50	−0.58	−20.93	−0.01
$(HF)_3$	C_{3h}	−31.07	−31.08	−31.24	−0.17	−25.50	−5.00	−0.63	−31.13	0.25
	D_{3h}	−30.52	−30.52	−29.64	0.88	−26.24	−4.00	0.01	−30.23	1.15
	$C_{\infty v}$	−31.73	−31.73	−30.67	1.06	−25.34	−5.24	−0.81	−31.38	0.00
$(HF)_4$	C_{4h}	−41.33	−41.33	−41.36	−0.03	−34.09	−6.54	−0.71	−41.34	0.50
	D_{4h}	−40.70	−40.70	−39.35	1.35	−34.74	−5.47	−0.03	−40.25	1.59
	$C_{\infty v}$	−42.26	−42.26	−40.90	1.36	−33.84	−6.96	−1.01	−41.81	0.03
$(HF)_5$	C_{5h}	−51.61	−51.61	−51.51	0.01	−42.64	−8.12	−0.82	−51.58	0.72
	D_{5h}	−50.87	−50.87	−49.17	1.70	−43.34	−6.93	−0.03	−50.30	2.00
	$C_{\infty v}$	−52.78	−52.78	−51.13	1.65	−42.35	−8.67	−1.21	−52.23	0.07
$(HF)_6$	S_6	−61.90	−61.89	−61.74	0.15	−51.16	−9.74	−0.95	−61.85	0.91
	C_{6h}	−61.92	−61.90	−61.70	0.21	−51.16	−9.74	−0.95	−61.84	0.92
	D_{6h}	−61.04	−61.06	−58.91	2.14	−51.97	−8.36	0.0	−60.33	2.43

Shown are the diagonal components $\chi_{\alpha\alpha}$, the anisotropy $\Delta\chi_{anis}$, diamagnetic (χ_{dia}), paramagnetic (χ_{para}), and nonlocal (χ_{nl}) components, the average value χ_m, and the diamagnetic exaltation Λ. All quantities given in the table are expressed in the irrational system $\chi_m^{(ir)}$ / (ppm cm^3 mol^{-1}). To convert to SI units, 1 ppm cm^3 mol^{-1} = 1 ppm cgs / mol = $4\pi 10^{-12}$ m^3 mol^{-1}. The magnetizability $\xi = m / B$ (ref. 135), which is the magnetic equivalent to the electric polarizability, can be obtained in the SI system via $\xi = \chi_m \mu_0^{-1} N_A^{-1}$, where μ_0 is the vacuum permeability and N_A the Avogadro number. Hence $\chi_m^{(ir)}$ / ppm cm^3 mol^{-1} ≈ 1.66054 · $10^{-29}\xi$ / (J T^{-2}) ≈ 0.2104 / ($e^2 a_0^2 / m_e$).[156] The gauge origin for the non-IGLO results was at the center of mass (c.m.) if not noted otherwise.

[a] $\Delta\chi_{anis} = \chi_{33} - 0.5(\chi_{11} + \chi_{22})$.

[b] $\Lambda = \chi_m(HF)_n) - n \cdot \chi_m(HF)$. Positive sign means reduced diamagnetic behavior.

[c] LDA with exchange only,[135] converted from magnetizabilities, see caption.

[d] LDA with exchange-correlation functional.[135]

[e] SCF values from (ref. 185).

[f] MP2 values from (ref. 185).

[g] Reference 186.

contact (FC) term in the IGLO-DFPT treatment.[190] Similarly, the experimental $^1J_{HF}$ in the bihalide anion FHF^- is $^1J_{HF}$ 120.5 ± 0.1 Hz in aprotic solvents,[191] compared to the computed value of 20 Hz. The development of more accurate functionals, which are especially designed for calculations of magnetic response properties, might resolve the current discrepancies.[190]

Conclusions

Hydrogen fluoride clusters are sufficiently elementary and well studied to serve as prototype systems for the investigation of hydrogen bonding[30,31] and hydrogen transfer.[192,193] Among the range of cluster sizes occurring in the normal vapor, the dimer is accessible to very high level quantum chemistry treatments; for large clusters one may look for viable alternative methods, such as density and hybrid functionals that we have investigated here. For structural and approximate energetic quantities, the BLYP density functional appears to be useful, although it exhibits disturbing deficiencies along the HF stretching and hydrogen transfer coordinates. It may provide the first reliable insights into the condensed phases of HF via the Car–Parrinello technique.[71] Alternative pure density functionals like the Becke–Roussel exchange functional[194] should also be examined.

TABLE XVI.
NICS Values (ppm, GIAO-SCF / 6 – 31 +G* // B3LYP / 6 – 311 + G) for $(HF)_n$ (n = 3 – 6) and Related Species.**

	C_{nh}	D_{nh}	
n	$(HF)_n$	$(HF)_n$	$(H_n)^{\pm q}$ [a]
3	−2.8	−5.6	−21.7
4	−1.1	−1.7	NA
5	−0.6	−0.8	−22.7
6	−0.4 (−0.35[b])	−0.5	−24.2[c]

[a] Data for D_{nh} symmetric H_3^+, H_5^-, and H_6, respectively, at GIAO-SCF / 6 −31 + G* // B3LYP / 6 −311 + + G(d, 3pd).
[b] S_6 symmetric ground state.
[c] Data taken from ref 187.

For accurate nuclear dynamics applications such as IR cluster size assignments, the deficiencies of pure density functionals are too large. They can be significantly reduced in hybrid approaches, among which we find the B3LYP functional to be generally superior to the BHHLYP functional. Variants of the B3LYP functional tailored to certain properties of HF lead to further improvements, but they are not flexible enough to remove the deficiencies in a fully satisfactory manner. Again, promising developments are underway in this field.[195, 196]

Currently, the price/performance ratio for *quantitatively reliable* HF cluster potential energy surfaces clearly remains best for the MP2 method (including MP2-R12),[43, 53] although slight systematic errors are noticeable even here.[43, 44, 53] However, the price for converged MP2 calculations is currently prohibitively high for larger clusters. Beyond the many-body decomposition approach, which we have applied successfully[17, 23] and which we are currently refining,[53] it would therefore be desirable to have an improved density or hybrid functional[196–198] for the problem at hand. Compared to the best functionals investigated in this work, such a functional should provide a better description of the monomer and considerably reduced complexation frequency shifts for the dimer and larger clusters.

Our judgment is based on a critical comparison to available experimental data, taking into account the strongly anharmonic, large amplitude quantum motion present in these hydrogen bonded clusters. Semiempirical methods[199] like the density functionals investigated here depend vitally on such a critical comparison in order to become useful instruments for the study of real systems. This provides an important incentive for our ongoing experimental characterization of HF clusters.

The present study may also serve as a convenient survey of our current theoretical knowledge of properties for larger $(HF)_n$ clusters where the experimental knowledge is still scarce (for an extension beyond $n = 6$, where weaker interactions than hydrogen bonding start to come into play, see (ref. 17). From the best theoretical estimates in the various tables, we may summarize the following main trends.

From the dimer $(HF)_2$ to the hexamer $(HF)_6$, the F ⋯ H hydrogen bond shrinks by about 15%, while the HF chemical bond is lengthened by about 3%. The hydrogen bond gains about a factor of 2 in strength (after inclusion of zero-point motion) and becomes essentially linear after overcoming the ring strain existing in the intermediate cluster sizes (n = 3–5, see Fig. 2). As a consequence, the energy required to evaporate one HF unit from the cold cluster reaches its peak for $(HF)_4$, where it may even slightly exceed the largest IR-active fundamental excitation. HF frequency shifts due to hydrogen bonding rise sharply with cluster size and level off smoothly with vanishing ring strain beyond $(HF)_5$. The barrier for concerted proton transfer between adjacent F atoms, for which only qualitative experimental evidence is available, is predicted to drop with increasing cluster size up to $(HF)_5$ (where it reaches an estimated zero-point corrected value of 20–140 kJ/mol[206] as compared to about 160–170 kJ/mol in the dimer), despite the growing number of protons that have to be transferred. Beyond $(HF)_5$, the latter effect causes an increase of the barrier. Irrespective of this pronounced loss of monomer identity in the larger clusters, there is no sign of cyclic electron delocalization.

Acknowledgments

We thank Wim Klopper, David Luckhaus, Ulrich Schmitt, and Jürgen Stohner for help and discussions and Kari Laasonen, Michele Parrinello, H.-J. Werner, and Sotiris Xantheas for discussions and correspondence. Various computer centers provided generous resources. The work in Zürich is supported financially by the Schweizerischer Nationalfonds and the ETH Zürich. The work in Erlangen was supported by the Deutsche Forschungsgemeinschaft. C. M. thanks the Fonds der Chemischen Industrie for a Kekulé scholarship.

References

1. B. J. Howard, T. R. Dyke, and W. Klemperer, *J. Chem. Phys.*, **81**, 5417 (1984).
2. A. S. Pine, W. J. Lafferty, and B. J. Howard, *J. Chem. Phys.*, **81**, 2939 (1984).
3. H. S. Gutowsky, C. Chuang, J. D. Keen, T. D. Klots, and T. Emilsson, *J. Chem. Phys.*, **83**, 2070 (1985).
4. A. S. Pine and B. J. Howard, *J. Chem. Phys.*, **84**, 590 (1986).
5. D. W. Michael and J. M. Lisy, *J. Chem. Phys.*, **85**, 2528 (1986).
6. K. v. Puttkamer and M. Quack, *Mol. Phys.*, **62**, 1047 (1987).
7. K. D. Kolenbrander, C. E. Dykstra, and J. M. Lisy, *J. Chem. Phys.*, **88**, 5995 (1988).
8. K. v. Puttkamer, M. Quack, and M. A. Suhm, *Mol. Phys.*, **65**, 1025 (1988).
9. K. v. Puttkamer and M. Quack, *Chem. Phys.*, **139**, 31 (1989).
10. H. Sun and R. O. Watts, *J. Chem. Phys.*, **92**, 603 (1990).
11. M. Quack and M. A. Suhm, *Chem. Phys. Lett.*, **171**, 517 (1990).
12. M. Quack and M. A. Suhm, *J. Chem. Phys.*, **95**, 28 (1991); M. Quack and M. A. Suhm in *Conceptual Perspectives in Quantum Chemistry*, *Vol. III*, E. S. Kryachko and J.-L. Calais, Eds., Kluwer, Dordrecht 1997, pp. 417–465.
13. R. E. Miller, *Acc. Chem. Res.*, **23**, 10 (1990).
14. M. A. Suhm, J. T. Farrell, Jr., A. McIlroy, and D. J. Nesbitt, *J. Chem. Phys.*, **97**, 5341 (1992).
15. M A. Suhm, J. T. Farrell, Jr., S. Ashworth, and D. J. Nesbitt, *J. Chem. Phys.*, **98**, 5985 (1993).
16. M. Quack, U. Schmitt, and M. A. Suhm, *Chem. Phys. Lett.*, **208**, 446 (1993).
17. M. Quack, J. Stohner, and M. A. Suhm, *J. Mol. Struct.*, **294**, 33 (1993), and to appear.
18. H.-C. Chang and W. Klemperer, *J. Chem. Phys.*, **100**, 1 (1994).
19. H.-C. Chang and W. Klemperer, *Faraday Discuss.*, **97**, 95 (1994).
20. R. J. Bemish, M. Wu, and R. E. Miller, *Faraday Discuss.*, **97**, 57 (1994).
21. D. J. Nesbitt, *Faraday Discuss.*, **97**, 1 (1994).
22. D. Luckhaus, M. Quack, U. Schmitt, and M. A. Suhm, *Ber. Bunsenges. Phys. Chem.*, **99**, 457 (1995).
23. M. A. Suhm, *Ber. Bunsenges. Phys. Chem.*, **99**, 1159 (1995).
24. D. H. Zhang, Q. Wu, J. Z. H. Zhang, M. von Dirke, and Z. Bačić, *J. Chem. Phys.*, **102**, 2315 (1995).
25. Q. Wu, D. H. Zhang, and J. Z. H. Zhang, *J. Chem. Phys.*, **103**, 2548 (1995).
26. R. Signorell, Y. He, H. B. Müller, M. Quack, and M. A. Suhm, In *Proceedings of the 10th International Symposium on Atomic, Molecular, Cluster, Ion, and Surface Physics*, J. P. Maier and M. Quack, Eds., Vdf Publishers, Zürich, 1996, p. 256.
27. R. G. Parr and W. Yang, *Density-Functional Theory of Atoms and Molecules*, Oxford University Press, Oxford, U.K., 1989.
28. R. G. Parr and W. Yang, *Annu. Rev. Phys. Chem.*, **46**, 701 (1995).
29. J. K. Labanowski and J. W. Andzelm, *Density Functional Methods in Chemistry*, Springer, Berlin, 1991.
30. P. Schuster, Ed., *Hydrogen Bonds, Topics in Current Chemistry Volume 120*, Springer, Berlin, 1984.
31. G. A. Jeffrey and W. Saenger, *Hydrogen Bonding in Biological Structures*, Springer, Berlin, 1991.
32. R. Ludwig, F. Weinhold, and T. C. Farrar, *J. Chem. Phys.*, **102**, 5118 (1995).
33. M. C. Holthausen, C. Heinemann, H. H. Cornehl, W. Koch, and H. Schwarz, *J. Chem. Phys.*, **102**, 4931 (1995).
34. A. v. d. Avoird, P. E. S. Wormer, and R. Moszynski, *Chem. Rev.*, **94**, 1931 (1994).
35. J. F. Gaw, Y. Yamaguchi, M. A. Vincent, and H. F. Schaefer, III, *J. Am. Chem. Soc.*, **106**, 3133 (1984).
36. S. Liu and C. E. Dykstra, *J. Phys. Chem.*, **90**, 3097 (1986).
37. M. Kofranek, H. Lischka, and A. Karpfen, *Chem. Phys.*, **121**, 137 (1988).
38. Z. Latajka and S. Scheiner, *Chem. Phys.*, **122**, 413 (1988).
39. P. Jensen, P. R. Bunker, A. Karpfen, M. Kofranek, and H. Lischka, *J. Chem. Phys.*, **93**, 6266 (1990).
40. A. Karpfen, *Int. J. Quantum Chem.* (*Quant. Chem. Symp.*), **24**, 129 (1990).
41. A. Karpfen and O. Yanovitskii, *J. Mol. Struct.* (*Theochem.*), **314**, 211 (1994).
42. J. J. Novoa, M. Planas, and M.-H. Whangbo, *Chem. Phys. Lett.*, **225**, 240 (1994).
43. K. A. Peterson and T. H. Dunning, Jr., *J. Chem. Phys.*, **102**, 2032 (1995).
44. C. L. Collins, K. Morihashi, Y. Yamaguchi, and H. F. Schaefer III, *J. Chem. Phys.*, **103**, 6051 (1995).
45. K. R. Liedl, R. T. Kroemer, and B. M. Rode, *Chem. Phys. Lett.*, **246**, 455 (1995), extended in this work.
46. M. J. Elrod and R. J. Saykally, *Chem. Rev.*, **94**, 1975 (1994).
47. G. Chałasinski and M. M. Szczęśniak, *Chem. Rev.*, **94**, 1723 (1994).
48. M. Tachikawa and K. Iguchi, *J. Chem. Phys.*, **101**, 3062 (1994).
49. F. H. Stillinger, *Int. J. Quant. Chem.*, **14**, 649 (1978).
50. A. Komornicki, D. A. Dixon, and P. R. Taylor, *J. Chem. Phys.*, **96**, 2920 (1992).
51. D. Heidrich, N. J. R. van Eikema Hommes, and P. von Ragué Schleyer, *J. Comput. Chem.*, **14**, 1149 (1993).
52. M. Quack and M. A. Suhm, *Chem. Phys. Lett.*, **183**, 187 (1991).
53. W. Klopper, M. Quack, and M. A. Suhm, *Chem. Phys. Lett.*, **261**, 35 (1996).
54. D. K. Hindermann and C. D. Cornwell, *J. Chem. Phys.*, **48**, 2017 (1968).
55. E. L. Mackor, C. MacLean, and C. W. Hilbers, *Recl. Trav. Chim.*, **87**, 655 (1968).
56. D. F. Smith, *J. Chem. Phys.*, **28**, 1040 (1958).
57. J. Simons and J. H. Hildebrand, *J. Am. Chem. Soc.*, **46**, 2183 (1924).
58. J. Janzen and L. S. Bartell, *J. Chem. Phys.*, **50**, 3611 (1969).
59. R. L. Redington, *J. Phys. Chem.*, **86**, 552 (1982).
60. E. U. Franck and F. Meyer, *Z. Elektrochemie*, **63**, 571 (1959).
61. S. Kristyán and P. Pulay, *Chem. Phys. Lett.*, **229**, 175 (1994).
62. M. L. Klein and I. R. McDonald, *J. Chem. Phys.*, **71**, 298 (1979).

63. M. E. Cournoyer and W. L. Jorgensen, *Mol. Phys.*, **51**, 119 (1984).
64. R. Car and M. Parrinello, *Phys. Rev. Lett.*, **55**, 2471 (1985).
65. D. K. Remler and P. A. Madden, *Mol. Phys.*, **70**, 921 (1990).
66. D. Marx and M. Parrinello, *J. Chem. Phys.*, **104**, 4077 (1996).
67. H.-P. Cheng, R. N. Barnett, and U. Landman, *Chem. Phys. Lett.*, **237**, 161 (1995).
68. M. Deraman, J. C. Dore, J. G. Powles, J. H. Holloway, and P. Chieux, *Mol. Phys.*, **55**, 1351 (1985).
69. K. Honda, K. Kitaura, and K. Nishimoto, *Bull. Chem. Soc. Jpn*, **65**, 3122 (1992).
70. D. A. Pinnick, A. I. Katz, and R. C. Hanson, *Phys. Rev. B*, **39**, 8677 (1989).
71. U. Röthlisberger and M. Parrinello, *J. Chem. Phys.* **106**, 4698 (1997).
72. N. C. Handy, C. W. Murray, and R. D. Amos, *J. Phys. Chem.*, **97**, 4392 (1993).
73. G. Rauhut and P. Pulay, *J. Phys. Chem.*, **99**, 3093 (1995).
74. M. J. Frisch, G. W. Trucks, H. B. Schlegel, P. M. W. Gill, B. G. Johnson, M. W. Wong, J. B. Foresman, M. A. Robb, M. Head–Gordon, E. S. Replogle, R. Gomperts, J. L. Andres, K. Raghavachari, J. S. Binkley, C. Gonzales, R. L. Martin, D. J. Fox, D. J. Defrees, J. Baker, J. P. Stewart, and J. A. Pople, *Gaussian 92/DFT*, Gaussian, Inc, Pittsburgh, PA, 1993.
75. M. J. Frisch, G. W. Trucks, H. B. Schlegel, P. M. W. Gill, B. G. Johnson, M. A. Robb, J. R. Cheeseman, T. Keith, G. A. Petersson, J. A. Montgomery, K. Raghavachari, M. A. Al-Laham, V. G. Zakrzewski, J. V. Ortiz, J. B. Foresman, J. Cioslowski, B. B. Stefanov, A. Nanayakkara, M. Challacombe, C. Y. Peng, P. Y. Ayala, W. Chen, M. W. Wong, J. L. Andres, E. S. Replogle, R. Gomperts, R. L. Martin, D. J. Fox, J. S. Binkley, D. J. Defrees, J. Baker, J. P. Stewart, M. Head–Gordon, C. Gonzales, and J. A. Pople, *Gaussian 94, Revision C.3*, Gaussian, Inc., Pittsburgh, PA, 1995.
76. J. Andzelm, In *Density Functional Methods in Chemistry*, J. K. Labanowski and J. W. Andzelm, Eds., Springer, Berlin, 1991, p. 155. DGauss is part of the UniChem system, which is a trademark of Cray Research, Inc.
77. K. Laasonen, M. Parrinello, R. Car, C. Lee, and D. Vanderbilt, *Chem. Phys. Lett.*, **207**, 208 (1993).
78. D. Vanderbilt, *Phys. Rev. B*, **41**, 7892 (1990).
79. K. Laasonen, M. Quack, and M. A. Suhm, unpublished results, (1990–1994).
80. J. P. Perdew, *Phys. Rev. B*, **33**, 8822 (1986).
81. A. D. Becke, *J. Chem. Phys.*, **96**, 2155 (1992).
82. A. D. Becke, *J. Chem. Phys.*, **98**, 5648 (1993).
83. A. D. Becke, *J. Chem. Phys.*, **98**, 1372 (1993).
84. M. Springborg, In *NATO ASI Series B: Proton Transfer in Hydrogen-Bonded Systems*, vol. 291, T. Bountis, Ed., Plenum, New York, 1992, p. 325.
85. B. G. Johnson, P. M. W. Gill, and J. A. Pople, *J. Chem. Phys.*, **98**, 5612 (1993).
86. Z. Latajka and Y. Bouteiller, *J. Chem. Phys.*, **101**, 9793 (1994).
87. J. E. DelBene, W. B. Person, and K. Szczepaniak, *J. Phys. Chem.*, **99**, 10705 (1995).
88. F. Mele, T. Mineva, N. Russo, and M. Toscano, *Theor. Chim. Acta*, **91**, 169 (1995), but see also ref. 160.
89. Y. Jeanvoine, F. Bohr, and M. F. Ruiz–López, *Can. J. Chem.*, **73**, 710 (1995).
90. P. Hobza, J. Sponer, and T. Reschel, *J. Comput. Chem.*, **16**, 1315 (1995).
91. J. J. Novoa and C. Sosa, *J. Phys. Chem.*, **99**, 15837 (1995).
92. C. Mijoule, Z. Latajka, and D. Borgis, *Chem. Phys. Lett.*, **208**, 364 (1993).
93. M. Weisser and W. Weyrich, *Z. Naturforsch. A*, **48**, 315 (1993).
94. R. V. Stanton and K. M. Merz, Jr., *J. Chem. Phys.*, **101**, 6658 (1994).
95. T. Zhu and W. Yang, *Int. J. Quantum Chem.*, **49**, 613 (1994).
96. H. Chojnacki, J. Andzelm, D. T. Nguyen, and W. A. Sokalski, *Comput. Chem.*, **19**, 181 (1995).
97. M. Tuckerman, K. Laasonen, M. Sprik, and M. Parrinello, *J. Phys. Chem.*, **99**, 5749 (1995).
98. (a) Z. Latajka, Y. Bouteiller, and S. Scheiner, *Chem. Phys. Lett.*, **234**, 159 (1995); (b) A. Karpfen, *J. Phys. Chem.*, **100**, 13474 (1996) and preprint; (c) G. Corongiu, D. Estrin, G. Murgia, L. Paglieri, L. Pisani, G. Suzzi Valli, J. D. Watts, and E. Clementi, *Int. J. Quantum Chem.*, **59**, 119 (1996); (d) L. Ojamäe, I. Shavitt, and S. J. Singer, *Int. J. Quantum Chem.: Quantum Chem. Symp.*, **29**, 657 (1995).
99. F. Sim, A. St.-Amant, I. Papai, and D. R. Salahub, *J. Am. Chem. Soc.*, **114**, 4391 (1992).
100. K. Laasonen, F. Csajka, and M. Parrinello, *Chem. Phys. Lett.*, **194**, 172 (1992).
101. K. Laasonen, M. Sprik, M. Parrinello, and R. Car, *J. Chem. Phys.*, **99**, 9080 (1993).
102. K. Laasonen and M. L. Klein, *J. Phys. Chem.*, **98**, 10079 (1994).
103. M. Kieninger and S. Suhai, *Int. J. Quantum Chem.*, **52**, 465 (1994).
104. R. Kaschner and G. Seifert, *Int. J. Quantum Chem.*, **52**, 957 (1994).
105. K. Kim and K. D. Jordan, *J. Phys. Chem.*, **98**, 10089 (1994).
106. J. Sauer, P. Ugliengo, E. Garrone, and V. R. Saunders, *Chem. Rev.*, **94**, 2095 (1994).
107. S. S. Xantheas, *J. Chem. Phys.*, **102**, 4505 (1995).
108. M. Sprik, J. Hutter, and M. Parrinello, *J. Chem. Phys.*, **105**, 1142 (1996).
109. D. M. Ceperley and B. J. Alder, *Phys. Rev. Lett.*, **45**, 566 (1980).
110. S. H. Vosko, L. Wilk, and M. Nusair, *Can. J. Phys.*, **58**, 1200 (1980).
111. J. P. Perdew and A. Zunger, *Phys. Rev. B*, **23**, 5048 (1981).
112. E. R. Davidson and S. J. Chakravorty, *Chem. Phys. Lett.*, **217**, 48 (1994).
113. J. E. DelBene and I. Shavitt, *J. Mol. Struct.* (*Theochem.*), **307**, 27 (1994).
114. C. Lee, W. Yang, and R. G. Parr, *Phys. Rev. B*, **37**, 785 (1988).
115. A. D. Becke, *Phys. Rev. A*, **38**, 3098 (1988).
116. F. Sim, D. R. Salahub, and S. Chin, *Int. J. Quantum Chem.*, **43**, 463 (1992).
117. M. M. Szczęśiak and G. Chałasinski, *J. Mol. Struct.* (*Theochem.*), **261**, 37 (1992).

118. T. N. Truong and W. Duncan, *J. Chem. Phys.*, **101**, 7408 (1994).
119. D. Wei and D. R. Salahub, *J. Chem. Phys.*, **101**, 7633 (1994).
120. J. Baker, J. Andzelm, M. Muir, and P. R. Taylor, *Chem. Phys. Lett.*, **237**, 53 (1995).
121. J. L. Durant, *Chem. Phys. Lett.*, **256**, 595 (1996).
122. C. Lee, D. Vanderbilt, K. Laasonen, R. Car, and M. Parrinello, *Phys. Rev. B*, **47**, 4863 (1993).
123. R. L. Bell and T. N. Truong, *J. Chem. Phys.*, **101**, 10442 (1994).
124. Q. Zhang, R. Bell, and T. N. Truong, *J. Phys. Chem.*, **99**, 592 (1995).
125. E. Ruiz, D. R. Salahub, and A. Vela, *J. Phys. Chem.*, **100**, 12265 (1996).
126. *DMol*, Biosym Technologies, Inc. San Diego, CA, 1991.
127. B. Delley, M. Wrinn, and H. P. Lüthi, *J. Chem. Phys.*, **100**, 5758 (1994).
128. D. Marx, J. Hutter, and M. Parrinello, *Chem. Phys. Lett.*, **241**, 457 (1995).
129. F. B. v. Duijneveldt, J. G. C. M. v. Duijneveldt−van de Rijdt, and J. H. v. Lenthe, *Chem. Rev.*, **94**, 1873 (1994).
130. J. M. L. Martin, E.-Y. Jamal, and J.-P. François, *Mol. Phys.*, **86**, 1437 (1995).
131. J. Andzelm and E. Wimmer, *J. Chem. Phys.*, **96**, 1280 (1992).
132. I. A. Topol, S. K. Burt, and A. A. Rashin, *Chem. Phys. Lett.*, **247**, 112 (1995).
133. P. M. W. Gill, B. G. Johnson, J. A. Pople, and M. J. Frisch, *Chem. Phys. Lett.*, **197**, 499 (1992).
134. N. S. Ostlund, M. D. Newton, J. W. McIver, Jr., and J. A. Pople, *J. Magn. Reson.*, **1**, 298 (1969).
135. A. M. Lee, S. M. Colwell, and N. C. Handy, *Chem. Phys. Lett.*, **229**, 225 (1994).
136. V. G. Malkin, O. L. Malkina, and D. R. Salahub, *Chem. Phys. Lett.*, **221**, 91 (1994).
137. J. Gauss, *Ber. Bunsenges. Phys. Chem.*, **99**, 1001 (1995).
138. J. Gauss and J. F. Stanton, *J. Chem. Phys.*, **104**, 2574 (1996).
139. P.-O. Astrand and K. V. Mikkelsen, *J. Chem. Phys.*, **104**, 648 (1996).
140. V. G. Malkin, O. L. Malkina, M. E. Casida, and D. R. Salahub, *J. Am. Chem. Soc.*, **116**, 5898 (1994).
141. (a) M. Schindler and W. Kutzelnigg, *J. Chem. Phys.*, **76**, 1919 (1982); (b) W. Kutzelnigg, *Israel J. Chem.*, **19**, 193 (1980).
142. W. Kutzelnigg, U. Fleischer, and M. Schindler, In *NMR Basic Principles and Progress*, vol. 23, P. Diehl, E. Fluck, H. Günther, R. Kosfeld, J. Seelig, Eds., Springer, Berlin, 1990, p. 165.
143. S. Huzinaga, *Approximate Wave Functions*, Univ. of Alberta, Edmonton, Alberta, Canada, 1971.
144. (a) A. St.-Amant and D. R. Salahub, *Chem. Phys. Lett.*, **169**, 387 (1990); (b) N. Godbout, D. R. Salahub, J. Andzelm, and E. Wimmer, *Can. J. Chem.*, **92**, 508 (1992).
145. J. P. Perdew and Y. Wang, *Phys. Rev. B*, **33**, 8800 (1986).
146. P. v. R. Schleyer and H. Jiao, *Pure Appl. Chem.*, **68**, 209 (1996).
147. H. J. Dauben, J. D. Wilson, and J. L. Laity, *J. Am. Chem. Soc.*, **90**, 811 (1968), **91**, 1991 (1969); H. J. Dauben, J. D. Wilson, and J. L. Laity. In *Nonbenzenoid Aromaticity*, vol. II, J. P. Snyder, Ed., 1971, pp. 167.
148. P. v. R. Schleyer, C. Maerker, A. Dransfeld, H. Jiao, and N. J. R. v. E. Hommes, *J. Am. Chem. Soc.*, 1996.
149. Leading GIAO-SCF references are (a) K. Wolinski, J. F. Hinton, and P. Pulay *J. Am. Chem. Soc.*, **112**, 8251 (1990); (b) R. Ditchfield, *Mol. Phys.*, **27**, 789 (1974); (c) H. Hameka, *Mol. Phys.*, **1**, 203 (1958).
150. J. Sauer, In *Proceedings of the 10th International Symposium on Atomic, Molecular, Cluster, Ion, and Surface Physics*, J. P. Maier and M. Quack, Eds., Verlag der Fachvereine, Zürich, 1996.
151. R. N. Sileo and T. A. Cool, *J. Chem. Phys.*, **65**, 117 (1976).
152. J. S. Muenter, *J. Chem. Phys.*, **56**, 5409 (1972).
153. J. Guan, P. Duffy, J. T. Carter, D. P. Chong, K. C. Casida, M. E. Casida, and M. Wrinn, *J. Chem. Phys.*, **98**, 4753 (1993).
154. B. G. Johnson and J. Flórian, *J. Chem. Phys.*, **98**, 5612 (1993).
155. S. A. C. McDowell, R. D. Amos, and N. C. Handy, *Chem. Phys. Lett.*, **235**, 1 (1995).
156. I. Mills, T. Cvitaš, K. Homann, N. Kallay, and K. Kuchitsu, *Quantities, Units and Symbols in Physical Chemistry*, Blackwell Scientific Publications, Oxford, U.K., 1993.
157. H.-J. Werner and P. Rosmus, *J. Chem. Phys.*, **73**, 2319 (1980).
158. J. M. L. Martin and P. R. Taylor, *Chem. Phys. Lett.*, **225**, 473 (1994).
159. W. Klopper, *J. Chem. Phys.*, **102**, 6168 (1995).
160. M. Quack and M. A. Suhm, *Theor. Chim. Acta*, **93**, 61 (1996).
161. J. T. Farrell, Jr., M. A. Suhm, and D. J. Nesbitt, *J. Chem. Phys.*, **104**, 9313 (1996).
162. M. Quack and M. A. Suhm, *Chem. Phys. Lett.*, **234**, 71 (1995).
163. D. T. Anderson, S. Davis, and D. J. Nesbitt, *J. Chem. Phys.*, **104**, 6225 (1996).
164. C. Laush and J. M. Lisy, *J. Chem. Phys.*, **101**, 7480 (1994).
165. F. Huisken, M. Kaloudis, A. Kulcke, and D. Voelkel, *Infrared Phys. Technol.*, **36**, 171 (1995).
166. H. Sun, R. O. Watts, and U. Buck, *J. Chem. Phys.*, **96**, 1810 (1992).
167. F. Huisken, E. G. Tarakanova, A. A. Vigasin, and G. V. Yukhnevich, *Chem. Phys. Lett.*, **245**, 319 (1995).
168. R. T. Lagemann and C. H. Knowles, *J. Chem. Phys.*, **32**, 561 (1960).
169. M. W. Johnson, E. Sandor, and E. Arzi, *Acta Cryst. B*, **31**, 1998 (1975).
170. S P. Habuda and Y. V. Gagarinsky, *Acta Cryst. B*, **27**, 1677 (1971).
171. M. A. Suhm and D. J. Nesbitt, *Chem. Soc. Rev.*, **24**, 45 (1995).
172. F. Huisken, M. Kaloudis, A. Kulcke, C. Laush, and J. M. Lisy, *J. Chem. Phys.*, **103**, 5366 (1995).
173. J. K. Gregory and D. C. Clary, *J. Chem. Phys.*, **103**, 8924 (1995).
174. T. Bürgi, T. Droz, and S. Leutwyler, *Chem. Phys. Lett.*, **246**, 291 (1995).
175. M. Quack and M. Suhm, In *Proceedings of the Symposium on Atomic, Cluster and Surface Physics '94*, T. Mářk, R. Schrittwieser, D. Smith, Eds., Maria Alm, 1994, p. 53.
176. R. W. Jansen, R. Bertoncini, D. A. Pinnick, A. I. Katz, R. C. Hanson, O. F. Sankey, and M. O'Keeffe, *Phys. Rev. B*, **35**, 9830 (1987).

177. C. Scheurer and P. Saalfrank, *J. Chem. Phys.*, **104**, 2869 (1996).
178. W. G. Schneider, H. J. Bernstein, and J. A. Pople, *J. Chem. Phys.*, **28**, 601 (1958).
179. C. Maerker, P. v. R. Schleyer, O. L. Malkina, V. G. Malkin, and D. R. Salahub, *J. Am. Chem. Soc.*, to appear.
180. J. P. Perdew and Y. Wang, *Phys. Rev. B*, **45**, 13244 (1992).
181. S. N. Smirnov, N. S. Golubev, G. S. Denisov, H. Benedict, P. Schah−Mohammedi, and H.-H. Limbach, *J. Am. Chem. Soc.*, **118**, 4094 (1996).
182. D. K. Hindermann and C. D. Cornwell, *J. Chem. Phys.*, **48**, 4142 (1968).
183. H. Jiao, P. v. R. Schleyer, and M. N. Glukhovtsev, *J. Phys. Chem.*, **100**, 12299 (1996).
184. (a) P. v. R. Schleyer, P. Freeman, H. Jiao, and B. Goldfuss, *Angew. Chem.*, **107**, 332 (1995); (b) H. Jiao and P. v. R. Schleyer, In *AIP Conference Proceedings 330, ECCC 1, Computational Chemistry*, F. Bernardi and J.-L. Rivail, Eds., AIP, Woodbury, NY, 1995, p. 107.
185. S. M. Cybulski and D. M. Bishop, *J. Chem. Phys.*, **100**, 2019 (1994).
186. P. Ehrlich, *Z. Anorg. Allg. Chem.*, **249**, 219 (1942).
187. H. Jiao and P. v. R. Schleyer, unpublished results.
188. The perturbation origin in the DFPT treatment was put on hydrogen if not otherwise noted. Fluorine as a perturbation site gives 5−7 Hz reduced Fermi-contact term data.
189. J. S. Muenter and W. Klemperer, *J. Chem. Phys.*, **52**, 6033 (1970).
190. (a) V. G. Malkin, O. L. Malkina, L. A. Eriksson, and D. R. Salahub, In *Modern Density Functional Theory: A Tool for Chemistry; Theoretical and Computatzonal Chemistry*, vol. 2, J. M. Seminario and P. Politzer, Eds., Elsevier, Amsterdam, 1995, p. 273; (b) O. L. Malkina, D. R. Salahub, and V. G. Malkin, *J. Chem. Phys.*, **105**, 8793 (1996).
191. J. S. Martin and F. Y. Fujiwara, *J. Am. Chem. Soc.*, **95**, 7632 (1974).
192. G. Zundel, *Topics Phys. Chem.*, **3**, 129 (1992).
193. F. Aguilar−Parrilla, G. Scherer, H.-H. Limbach, M. d. l. C. Foces−Foces, F. H. Cano, J. A. S. Smith, C. Toiron, and J. Elguero, *J. Am. Chem. Soc.*, **114**, 9657 (1992).
194. R. Neumann and N. C. Handy, *Chem. Phys. Lett.*, **246**, 381 (1995).
195. V. E. Ingamells and N. C. Handy, *Chem. Phys. Lett.*, **248**, 373 (1996).
196. R. Neumann and N. C. Handy, *Chem. Phys. Lett.*, **252**, 19 (1996).
197. E. I. Proynov, E. Ruiz, A. Vela, and D. R. Salahub, *Int. J. Quantum Chem.: Quantum Chem. Symp.*, **29**, 61 (1995).
198. A. D. Becke, *J. Chem. Phys.*, **104**, 1040 (1995).
199. W. D. Chandler, K. E. Johnson, and J. L. E. Campbell, *Inorg. Chem.*, **34**, 4943 (1995).
200. K. P. Huber and G. Herzberg, *Molecular Spectra and Molecular Structure. IV. Constants of Diatomic Molecules*, Van Nostrand Reinhold, New York, 1979.
201. S. M. Bass, R. L. DeLeon, and J. S. Muenter, *J. Chem. Phys.*, **86**, 4305 (1987).
202. A. A. Rashin, L. Young, I. A. Topol, and S. K. Burt, *Chem. Phys. Lett.*, **230**, 182 (1994).
203. K. v. Puttkamer, M. Quack, and M. A. Suhm, *Infrared Phys.*, **29**, 535 (1989).
204. M. Atoji and W. N. Lipscomb, *Acta Crystallogr.*, **7**, 173 (1954).
205. A. E. Reed, F. Weinhold, L. A. Curtiss, and D. J. Pochatko, *J. Chem. Phys.*, **84**, 5687 (1986).
206. W. Klopper, M. Quack, and M. A. Suhm, to be published.